Understanding the DayCent model: Calibration, sensitivity, and identifiability through inverse modeling

Magdalena Necpálová [a, *], Robert P. Anex [a], Michael N. Fienen [b], Stephen J. Del Grosso [c], Michael J. Castellano [d], John E. Sawyer [d], Javed Iqbal [d], José L. Pantoja [d], Daniel W. Barker [d]

[a] Department of Biological System Engineering, University of Wisconsin–Madison, Madison, WI, USA
[b] United States Geological Survey, Wisconsin Water Science Center, Middleton, WI, USA
[c] Natural Resource Ecology Laboratory, Colorado State University, Fort Collins, CO, USA
[d] Dept. of Agronomy, Iowa State University, Ames, IA, USA

ARTICLE INFO

ABSTRACT

The ability of biogeochemical ecosystem models to represent agro-ecosystems depends on their correct integration with field observations. We report simultaneous calibration of 67 DayCent model parameters using multiple observation types through inverse modeling using the PEST parameter estimation software. Parameter estimation reduced the total sum of weighted squared residuals by 56% and improved model fit to crop productivity, soil carbon, volumetric soil water content, soil temperature, N_2O, and soil NO_3^- compared to the default simulation. Inverse modeling substantially reduced predictive model error relative to the default model for all model predictions, except for soil NO_3^- and NH_4^+. Post-processing analyses provided insights into parameter–observation relationships based on parameter correlations, sensitivity and identifiability. Inverse modeling tools are shown to be a powerful way to systematize and accelerate the process of biogeochemical model interrogation, improving our understanding of model function and the underlying ecosystem biogeochemical processes that they represent.

Software and data availability section

Software DayCent model
Developers W. J. Parton, S. J. Del Grosso, S. Ogle, K. Paustian,
Contact address Natural Resource Ecology Laboratory,
  Colorado State University, Fort Collins, CO,
  USA
Telephone (970) 491-2195
Email address century@colostate.edu
Year first available 1998
Hardware required PC with at least 512 K of RAM. A graphics adapter (CGA, EGA, VGA, or Hercules monographic) and 2 Mb of disk space are recommended.
Software required Windows
Availability and cost Available on request; Free
Software PEST version 13.0
Developer John Doherty
Contact address Watermark Numerical Computing, 336 Cliveden Avenue, Corinda 4075, Australia
Telephone 07 3379 1664
Email address johndoherty@ozemail.com.au

Year first available	1994
Hardware required	Desktop or Laptop
Software required	Windows or Linux
Availability and cost	down load from: http://www.pesthomepage.org/Downloads.php; Free.

1. Introduction

Greenhouse gases (GHG) released from the soils of terrestrial ecosystems are highly variable in space and time due to the inter-action of climatic drivers and ecosystem processes involved in carbon (C) and nitrogen (N) transformation associated with production and consumption of GHGs (Müllera et al., 2002; Rahn et al., 2012; Wrage et al., 2001). Field measurements that capture the high temporal and spatial variability of N_2O fluxes (Bouwman et al., 2002; Parkin, 2008; Snyder et al., 2009) or the high spatial variability of soil organic carbon (SOC; Conant and Paustian, 2002; Kravchenko and Robertson, 2011) are expensive, time intensive, and unable to capture the full range of ecological and environmental conditions. When properly informed by field observations, ecosystem process-based models are a powerful way to investigate the effects of management practices on GHG emissions or SOC from different ecosystems, soils, and climates.

A number of biogeochemical models have been developed and used to quantify GHG emissions and SOC at both plot and landscape scales, e.g., Century (Parton et al., 1994; Parton, 1996), DayCent (Del Grosso et al., 2005; Parton et al., 1998), deni-trification–decomposition (DNDC) (Li et al., 2000), ecosys (Grant et al., 1993) and EPIC (Wang, 2005). These models are mathematical representations of our understanding of the complicated, coupled biogeochemical soil processes that allow us to test our understanding through comparison of model results with observations, and predict responses to conditions that have not yet been observed, such as ecosystem responses to changing climate. Thus these models have become important tools in the study of biogeochemical cycles. Model development is based on a quantitative understanding of the interactions among physical, chemical and biological processes that is critical for predicting the ecosystem response to land use or climate change. The individual underlying processes are represented by sets of equations in component models that are coupled together to describe a full system (Wallach et al., 2014). Models usually have a mechanistic structure that reflects our understanding of the processes governing the system behavior. Many ecosystem models utilize several hundred parameters representing individual physical quantities or combinations of physical quantities that may not be observable through direct measurement. It is thus impossible to measure the sensitivity of system behavior to each of these parameters and information on their identifiability through field observations is often not available. Yet for model users and particularly model developers, an understanding of how model parameters influence the simulation of target ecosystem processes and which field observations are most useful in defining parameter values is essential.

The DayCent model is a widely used terrestrial biogeochemical process-based model of intermediate complexity (Del Grosso et al., 2001, 2002; Parton et al., 1998). It has been used to simulate ecosystem responses to changes in climate and agricultural management practices in crop, grassland, forest and savanna ecosystems (Brilli et al., 2013; Cheng et al., 2014; Del Grosso et al., 2008a, 2009; Hartman et al., 2009; Parton et al., 2007; Parton and Rasmussen, 1994). In the USA, it has been used to quantify N_2O emissions from agricultural soils for the US National Greenhouse Gas Inventory compiled by the EPA (Olander and Haugen-Kozyra, 2011) and reported annually to the UN Framework Convention on Climate Change (US EPA, 2014). DayCent consists of sub-models for soil water content and temperature by layer, plant production and allocation of net primary production (NPP), decomposition of litter and soil organic matter (SOM), mineralization of nutrients, N gas emissions from nitrification and denitrification, and CH_4 oxidation in unsaturated soils.

The accuracy with which a model represents the natural system observed in the field depends on how completely the underlying biophysical processes are represented in the model and how well the model parameters are calibrated to field observations. Like other biogeochemical process-based models, DayCent is typically calibrated manually by adjusting one parameter at a time, thus the calibrated parameters are adjusted in an iterative fashion in multiple stages (Wallach et al., 2014). At each stage, specific processes are targeted (e.g., plant growth and yield, SOC), and the most influential parameters are adjusted to match simulated to observed values (Del Grosso et al., 2011). This approach, however, does not guarantee full extraction of information from the field observations and it is difficult to know when calibration correctly balances the performance of all model components (Nolan et al., 2011). It is generally accepted that manual calibration of complex ecosystem models does not necessarily yield optimal parameter estimates, is somewhat arbitrary, and results in high uncertainty in model parameters and simulated variables (Schwarz et al., 2006). Inverse modeling, based on an objective statistical method and mathematical techniques for stable parameter estimation, has become a widely accepted way to enhance the transfer of information contained in field observations to model parameters (Doherty, 2003; Doherty and Hunt, 2010a; Hunt et al., 2007). Despite mathematical objectivity, some subjectivity is unavoidable: through defining the conceptualization of the inverse problem and making a set of decisions related to regularization, parameter bounds, observation weighting strategy, etc. (Fienen, 2013). The inverse modeling tool PEST (Doherty, 2010) uses an iterative, nonlinear regression approach that involves simultaneous adjustment of multiple model parameters and evaluation of model fit by the sum of weighted squared residuals between field observations and simulated values. In addition to providing sophisticated estimates of the parameter values that provide the best possible fit for a given calibration problem, inverse modeling provides a method for comprehensive model analysis through statistical measures such as the variance/covariance matrix, parameter correlations, confidence intervals, sensitivities, identifiability, and predictive uncertainty analysis (Moore and Doherty, 2005, 2006).

These tools can help users recognize model problems that are difficult to identify with manual calibration methods (Hill and Tiedeman, 2007; Poeter and Hill, 1997). For example, it has been repeatedly observed that only a small number of the many parameters used in most environmental models are uniquely estimable with most datasets (Beck and Halfon, 1991; Beven and Freer, 2001; Doherty and Hunt, 2009). The inability to uniquely identify certain model parameters can be the result of their high correlation with other parameters, or lack of sensitivity of the model outputs to these parameters. This sort of problem is extremely difficult to recognize without specialized tools and can lead to misidentification of parameter values, model over-fitting, and inaccurate model projections for conditions outside the range of the calibration dataset. Applying inverse modeling tools provides valuable insight about parameter dependencies, which parameters are exerting the most influence on the simulated values, whether the field observations contain enough information to estimate the model parameters, and the uncertainty associated with the predictions based on the estimated parameter values.

Inverse modeling has been applied to soil physics and ground-water studies where inverse simulations are commonly used to parameterize hydraulic functions (e.g., Bitterlich et al., 2005; Kosugi et al., 2001; Lin and Anderson, 2003; Spohrer et al., 2006; Tonkin and Doherty, 2009). It has been also applied to three biogeochemical models, i.e. RZWQM (Malone et al., 2010, 2014; Nolan et al., 2010) to calibrate soil hydraulic, N leaching, N transformation and crop yield parameters; Forest DNDC (Lamers et al., 2007) and DayCent (Rafique et al., 2013) to calibrate parameters associated with C and N trace gas production. These studies performed calibration with a reduced number of degrees of freedom to increase efficiency. To our knowledge, no previous study has demonstrated the full use of inverse modeling by calibrating multiple components of an ecosystem biogeochemical model and explicating model function through the use of associated sensitivity and identifiability methods.

The objectives of this study were to demonstrate calibrating the major components of the DayCent model with several types of field observations simultaneously through inverse modeling as implemented in the PEST parameter estimation software (Doherty, 2010), and to provide insights into the function of the model. Outputs simulated using the estimated parameter values were validated against an independent dataset. Using parameter correlations, sensitivity and identifiability we provide insights into the complex DayCent model structure and explore the relationships between model parameters and observations.

2. Material and methods

2.1. Study location and data

The study was conducted at Iowa State University Agricultural Engineering and Agronomy Ames Research Farm (42.01N, 93.78W). Long term mean annual temperature and rainfall are 9.4 °C and 827 mm yr^{-1}. The soil is predominantly Clarion loam series (fine loamy, mixes, superactive, mesic Typic Hapludolls) with pH 6.62, cation-exchange capacity (CEC) 20.38, SOC content of 23.3 g kg^{-1}, total N content 1.77 g kg^{-1} soil at 0–10 cm. The soil texture is loam and clay loam (39.5% sand and 38.2% silt at 0–10 cm).

SOC, crop aboveground net primary productivity (ANPP), grain yields, soil NO_3^-, NH_4^+, N_2O emissions, soil temperature and volumetric soil water content (VSWC) were measured over a 3 year period (2011–2013) as part of a field experiment studying the effect of winter rye cover crop on soil N_2O emissions from a corn–soybean cropping system treated with different N fertilizer rates. A detailed description of the sampling strategy and analytical procedures has been reported by Mitchell et al. (2013) and Kladivko et al. (2014). This study used one treatment with N rate of 135 kg N fertilizer ha^{-1}, no cover crop, managed without tillage. During the corn phase, N fertilizer was applied as urea ammonium nitrate (UAN, 32% N), side-dressed in bands at 15 cm depth. All the data, except for SOC and crop ANPP, were collected from the fertilizer bands which were, on an area basis, calculated to have received twice the N fertilizer of surrounding areas. Weather data were collected from a meteorological station. The site received 815.3, 692.4, and 852.1 mm of

rainfall in 2011, 2012, and 2013, respectively. The mean air temperature was 10.0 °C in 2011, 11.6 °C in 2012, and 8.5 °C in 2013 (Fig. 1).

2.2. DayCent modeling

DayCent is a terrestrial ecosystem model designed to simulate fluxes of C and N among the atmosphere, vegetation, and soil (Del Grosso et al., 2001; Parton et al., 1998). DayCent is the daily time-step version of the Century model (Parton et al., 1994). The plant growth submodel simulates plant productivity as a function of genetic potential, phenology, nutrient availability, water/temperature stress, and solar radiation (i.e. energy biomass conversion factor). NPP is allocated to plant components (e.g., roots vs. shoots) based on vegetation type, phenology, and water/nutrient stress. Nutrient concentrations of plant components vary within specified limits depending on vegetation type and nutrient availability relative to plant demand (Del Grosso et al., 2008a). SOM is simulated in the top 20 cm soil layer as a sum of dead plant matter and three SOM pools (active, slow, and passive) on the basis of decomposition rates. The amount of biomass decomposition products entering the pools and flowing between the pools depend on lignin content and C/N ratio, size of the pools, temperature/water factors, and clay content (Del Grosso et al., 2001, 2011; Parton et al., 1994). The decomposition of litter, SOM, and nutrient mineralization are functions of substrate availability, lignin content, C/N ratio, water/temperature stress, and tillage intensity (Del Grosso et al., 2008a). The trace gas model contains both denitrification and nitrification submodels. Daily denitrification rates are calculated for each soil layer based on soil NO_3^- concentration distributed throughout the soil profile, heterotrophic respiration (i.e., available labile C), soil water content, texture, and temperature; while nitrification rates are calculated based on soil NH_4^+ concentration, water content, texture, and the temperature in the top 15 cm layer (Del Grosso et al., 2001, 2008a; Parton et al., 2001). The soil water sub-model simulates soil water content and water fluxes (i.e., through the canopy, surface run off, leaching, evaporation and transpiration) throughout the defined depth of the soil profile (Parton et al., 1998). When the average daily air temperature is freezing, the precipitation is accumulated in the snowpack. Saturated water flow occurs on days that receive rainfall, irrigation, or snow melt every day on a sub-daily time step (Del Grosso et al., 2008a). Each soil layer is filled before water flows to the next layer and if the input rate is greater than saturated hydraulic conductivity, the difference goes into surface runoff (Del Grosso et al., 2001). Unsaturated flow simulated by tipping bucket method is calculated using Darcy's law as a function of the hydraulic conductivity of soil layers and the difference in hydraulic potential calculated for the centers of adjacent soil layers. The flux from the top layer depends on potential evapotranspiration rate, water content of the top soil layer, and the minimum water content set for the top layer (Del Grosso et al., 2001). Soil NO_3^- is distributed throughout the soil profile and available for leaching into the subsoil. Its movement and leaching are largely controlled by soil water flow and plant N uptake. The nitrification sub-model modifies soil NH_4^+ concentration which is assumed to be immobile and distributed entirely in the top 15 cm layer of soil (Del Grosso et al., 2008a).

DayCent version 4.5 was used to simulate SOC, crop ANPP, N_2O fluxes and soil NO_3^- and NH_4^+ at the plot scale representing the area of the plot (6.1 × 15.2 m). The initial SOC pools were generated and stabilized using a "spin-up" simulation of native prairie ecosystem (mix of perennial C3 warm and cold grasses species and symbiotic N_2 fixing plants), and naturally occurring disturbances (1000–1800) followed by simulation of historical land cover/use data (i.e., grazing until 1880, low fertilized corn–wheat-fallow rotation followed by more intensive corn–soybean rotations) and current management (2010–2020). The dates of the current management events such as planting/harvest, and fertilizer application were consistent with the operations in the fields during 2011–2013. The simulation was driven using site-specific measured weather data (i.e., daily rainfall, high and low air
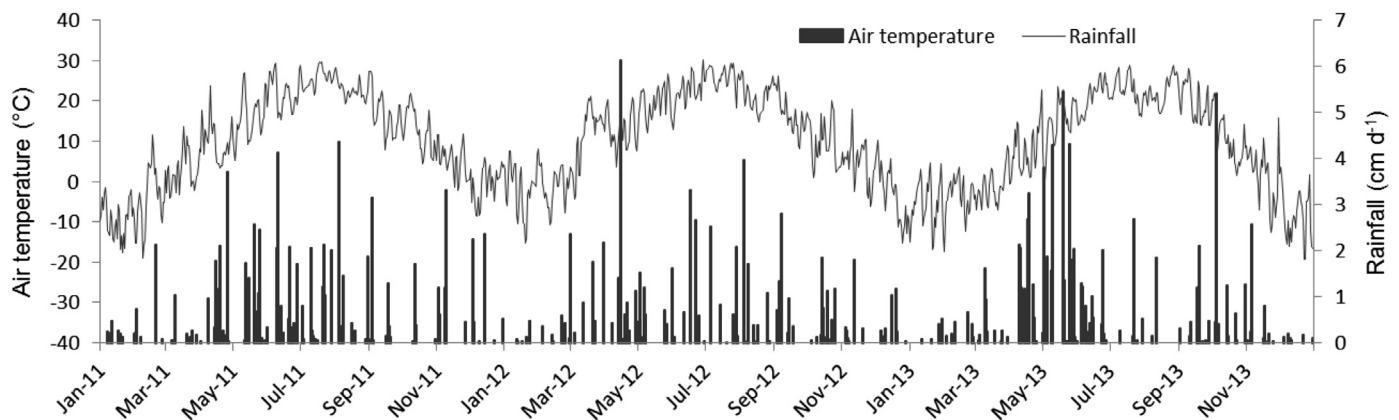

Fig. 1. Daily air temperature and rainfall during calibration (2011–2012) and validation period (2013).

temperatures) from 1950 to 2012, which were used repeatedly over the course of simulation. Simulation soil profile comprising of 13 soil layers (0—180 cm) was characterized by plot specific soil texture, SOC, bulk density and pH measured at 0—10, 10—20, 20—40, and 40—60 cm depth. The field capacity, wilting point, and saturated hydraulic conductivity for each depth were calculated using the Soil Water Characteristics Calculator software (SWCC), version 6.02.74 (USDA Agricultural Research Service, Washington). "Default simulation" here refers to simulation using site specific soil and weather data with all model parameters set to their default values as defined by the model developers. The model was calibrated using field observations, described above, for years 2011 and 2012, and validated against data collected in 2013 (Table 1).

2.3. Inverse modelling

Inverse modelling of DayCent parameters was accomplished using a model-independent parameter estimation software package PEST (Doherty, 2010). PEST allows independent parameter estimation using a nonlinear regression method grounded in the principles of least-squares minimization (Doherty and Hunt, 2010a); i.e. the model parameters are estimated in an iterative fashion as the code systematically varies model inputs, runs the model, reads model output, and evaluates the model fit using an objective function, which represents weighted least squared difference between observations and simulated values (Doherty, 2010), expressed as

$$\phi(\mathbf{b}) = [\mathbf{y} - \mathbf{y}\prime(\mathbf{b})]^T \, \mathbf{Q} \left[\mathbf{y} - \mathbf{y}\prime(\mathbf{b})\right]$$

where $\mathbf{Q}$ is a diagonal matrix with the squared observation weights on the diagonal, $\mathbf{y}$ is a vector of observations, $\mathbf{y}\prime(\mathbf{b})$ is a vector of model outputs from the DayCent model, based on parameter vector $\mathbf{b}$, and collocated with the observations in $\mathbf{y}$, and T indicates matrix transpose. The symbology is adopted from Nolan et al. (2011). Parameters that minimize this equation are obtained by solving the normal equations using the Gauss—Marquardt—Levenberg (GML) gradient search algorithm. At the start of each iteration, the relationship between the model parameters and the model-generated outputs is linearized through formulation as a Taylor expansion based on the current best parameter set. The matrix of all first-order partial derivatives of the simulated values that correspond to observations in the calibration dataset to the adjustable model parameters (i.e., the "Jacobian") is computed using the finite difference method. The linearized problem is then solved for a better parameter set using the GML algorithm, and the new parameters are tested by running the model and computing the objective function as defined above. The parameter changes and objective function improvement are compared with those of the previous iteration to determine if another iteration is justified. If it is, the entire process is repeated; if not, the parameter estimation process terminates (Doherty, 2010).

The calibration dataset comprises 111 field observations (Table 1). A weighted multicomponent objective function was adopted, similar to that used in Nolan et al. (2011) and Lin and Radcliffe (2006). Each observation type was assigned to a different observation group, and each observation group formed a component of the objective function which was representative of that type of observation (e.g., soil temperature measurements). An inter-group weighting strategy was defined using PEST utility PWTADJ1 (Doherty and Welter, 2010) such that each group contributed equally to the objective function at the start of the estimation process. This ensures that each observation group contributes information to the process, regardless of number of observations per group, units of measure, and other confounding factors. Individual field observations were weighted equally within each group.

Prior to the parameter estimation process, field capacity and wilting point in the DayCent input soil file were adjusted as described by Del Grosso et al. (2011).

Parameters included in inverse modeling (Table 2) were selected based on our prior knowledge of the model as being influential in the DayCent submodels. The default parameter values were used as initial values and upper and lower bounds were specified by one of the DayCent developers (personal communication, S. Del Grosso and B. Parton, December 6, 2013, Table 2). All parameters were log-transformed to strengthen the linear relationships between parameters and simulated values (Doherty and Hunt, 2010a). Numerical stability of inverse modeling was ensured through regularization using truncated singular value decomposition (SVD) of the weighted Jacobian matrix on an iteration-by-iteration basis. The level of truncation was automatically calculated based on a stability criterion. This regularization method transforms the original model parameters into linear combinations (i.e., eigenvectors), determines which are most sensitive (Moore and Doherty, 2005; Tonkin and Doherty, 2005), and truncates the transformed normal equations matrix, reducing the number of estimated parameters to maintain numerical stability and maximum reasonableness (Aster et al., 2005). The resulting regularized inversion process will not include parameters that are unidentifiable with the available data. When correlated parameters are included in the inversion, the SVD-based regression finds the maximum likelihood combination of the parameters that is consistent with the observations.

Details of the process of coupling the PEST software with DayCent model have been reported by Rafique et al. (2013). The runtime of the parameter estimation process was decreased through use of the BeoPEST version of PEST designed for parallel processing on a distributed grid of processors (Hunt et al., 2010; Schreuder, 2009).

Pre-calibration parameter correlations were obtained from the correlation coefficient matrix by using a standard Gauss—Marquardt—Levenberg parameter-estimation method. Relative composite sensitivity of each parameter with respect to each observation group and to the entire calibration dataset at the beginning of the parameter estimation process was computed as the magnitude of the column of the Jacobian matrix corresponding to the i_{th} parameter with each entry in that column multiplied by the squared weight associated with the corresponding observation, multiplied with the absolute value of the parameter value (Doherty, 2005):

$$s_i = \left(\mathbf{J}^T \mathbf{Q} \mathbf{J}\right)_{ii}^{1/2} {}^* \left|v_i\right|$$

where $\mathbf{J}$ is the Jacobian matrix and $\mathbf{Q}$ is a diagonal matrix whose elements are comprised of the squared observation weights and $|v_i|$ is the absolute value of the parameter value. Parameters with relative composite sensitivity >10% of the maximum relative composite sensitivity obtained for the set of parameters were considered to be highly sensitive, while parameters with relative composite sensitivity <1% were considered to be insensitive to the inversion problem (Hill and Tiedeman, 2007). The sensitivity analysis was used as a diagnostic of the inverse process, not as a standalone analysis. Therefore, the initial values and the assumptions were consistent with those used in the inversion.

Parameter identifiability, which represents the ability of a calibration dataset to constrain model parameters (Doherty and Hunt, 2009), was calculated through SVD of the weighted Jacobian matrix computed on the basis of initial parameter values. The boundary between the solution and null subspaces was set at a specific singular value calculated using the SUPCALC utility (Doherty, 2008) as described by Doherty and Hunt (2009). The number of singular vectors used to compute identifiability differed between the observation groups from 5 to 11 by means of the different number of field observations. The identifiability of the i_{th} parameter was calculated as a sum of the squared i_{th} components of all eigenvectors spanning the calibration solution space ($\mathbf{V_1}$) (Doherty, 2010):

$$Id_i = \Sigma(\mathbf{V}_{1i})^2$$

Table 1

Field observations included in DayCent calibration using an inverse modeling approach. Sampling strategy and analytical procedures were described by Mitchell et al. (2013) and Kladivko et al. (2014).

Observation group	N	Units	Data source	Sampling frequency
Crop productivity	3	g C m^{-2}	Grain yield was determined by combine harvesters. ANPP was determined on 6 plants and upscaled on an area basis through plant population. Subsamples for C were analyzed by dry combustion.	Once a year
Soil organic carbon	1	mg C kg^{-1} soil	Soil core analyzed for C by dry combustion	Once over the study period
N$_2$O soil emissions	24	g N$_2$O— N ha^{-1} d^{-1}	Static chamber inserted into 5-cm depth, analyzed in situ with a 1412 Infrared Photoacoustic Gas Monitoring System	Once a week
Volumetric soil water content	23	cm^3 cm^{-3}	Content to 5 cm depth measured with a TH300 theta probe	
Soil NO$_3$$^-$—N concentration	19	mg NO$_3$–N kg^{-1} soil	Soil cores to 10 cm depth extracted in 2 M KCl and analyzed in microplates using the Griess—Ilosvay reaction	Once a week
Soil NH$_4$$^+$—N concentration	17	mg NH$_4$–N kg^{-1} soil	Soil cores to 10 cm depth extracted in 2 M KCl and analysed in microplates using the Griess—Ilosvay reaction	Once a week
Soil temperature	24	°C	At 5 cm depth measured with a thermometer	Once a week

Table 2
DayCent adjustable parameters used in inverse modeling as they are defined in Metherell et al. (1993); their initial parameter values, upper and lower bounds compared to final estimated parameter values.

Parameter	Description	Units	Initial value	Lower bound	Upper bound	Estimated value
aneref(1)	Ratio of rain/potential evapotranspiration below which there is no negative impact of soil anaerobic conditions on decomposition	unitless	1.5	1	2	1
aneref(2)	Ratio of rain/potential evapotranspiration above which there is maximum negative impact of soil anaerobic conditions on decomposition	unitless	3	2.8	5	5
aneref(3)	Minimum value of the impact of soil anaerobic conditions on decomposition; functions as a multiplier for the maximum decomposition rate	unitless	1	0.2	1.1	0.2
basef	The fraction of the soil water content of layer NLAYER+1 which is lost via base flow	fraction H_2O	0.3	0.1	0.5	0.1
cfrtcn(1)	Maximum fraction of C allocated to roots under maximum nutrient stress	fraction NPP	0.6	0.51	0.8	0.51
cfrtcn(2)	Minimum fraction of C allocated to roots with no nutrient stress	fraction NPP	0.4	0.2	0.49	0.49
cfrtcw(1)	Maximum fraction of C allocated to roots under maximum water stress	fraction NPP	0.75	0.56	1	1
cfrtcw(2)	Minimum fraction of C allocated to roots with no water stress	fraction NPP	0.35	0.2	0.54	0.2
damr(1,1)	Fraction of surface N absorbed by residue	fraction N	0.02	0.002	0.3	0.002
damrmn(1)	Minimum C/N ratio allowed in residue after direct absorption	C/N	15	5	30	5
dec1(1)	Maximum surface structural decomposition rate, the fraction of the pool that turns over each year	g C per month	3.9	3	5	5
dec1(2)	Maximum soil structural decomposition rate, the fraction of the pool that turns over each year	g C per month	4.9	3	7	3
dec2(1)	Maximum surface metabolic decomposition rate, the fraction of the pool that turns over each year	g C per month	14.8	12	18	18
dec2(2)	Maximum soil metabolic decomposition rate, the fraction of the pool that turns over each year	g C per month	18.5	16	21	16
dec3(1)	Maximum decomposition rate of surface organic matter with active turnover, the fraction of the pool that turns over each year	g C per month	6	4	8	7.84
dec3(2)	Maximum decomposition rate of soil organic matter with active turnover, the fraction of the pool that turns over each year	g C per month	7.3	5	10	5
dec4	Maximum decomposition rate of soil organic matter with slow turnover, the fraction of the pool that turns over each year	g C per month	0.0025	0.002	0.03	0.03
dec5(2)	Maximum decomposition rate of soil organic matter with intermediate turnover, the fraction of the pool that turns over each year	g C per month	0.12	0.1	0.2	0.1
dmp_st	Damping factor for calculating soil temperature by layer	unitless	0.003	0.001	0.01	0.002
dmpflux	The damping factor for soil water flux is a multiplier used to reduce (or dampen) the upward and downward soil water fluxes between two soil layers in a Darcy's Law calculation. Without this multiplier, large gradients in the calculated soil water matric potential between adjacent soil layers can cause unrealistically high soil water flux rates.	unitless	0.000008	0.000001	0.0001	0.0001
drain	The fraction of excess water lost by drainage; indicates whether a soil is sensitive for anaerobiosis (drain = 0) or not (drain = 1)	fraction H_2O	1	0.2	1	0.9
epnfa(1)	Intercept value for determining the effect of annual precipitation on atmospheric N fixation (wet and dry deposition)	g N/m^2/yr/cm precip	0.3	0.02	0.5	0.02
epnfa(2)	Slope value for determining the effect of annual precipitation on atmospheric N fixation (wet and dry deposition)	g N/m^2/yr/cm precip	1.50E-02	0.002	0.5	0.137
epnfs(1)	Minimum AET value used for determining the effect of annual evapotranspiration on non-symbiotic soil N fixation; not used if nsnfix = 1	cm	30	10	40	40
epnfs(2)	Intercept value for determining the effect of annual evapotranspiration non-symbiotic soil N fixation; not used if nsnfix = 1	g N/m2/yr/cm aet	1.00E-02	0.001	0.1	0.1
favail(1)	Fraction of N available per month to plants	fraction N	0.15	0.1	0.5	0.1
fleach(1)	Intercept value for a normal month to compute the fraction of mineral N, P, and S which will leach to the next layer when there is a saturated water flow; normal leaching is a function of sand content	fraction N	0.5	0.001	1	0.38
fleach(2)	Slope value for a normal month to compute the fraction of mineral N, P, and S which will leach to the next layer when there is a saturated water flow; normal leaching is a function of sand content	fraction N	0.5	0.001	1	1
fleach(3)	Leaching fraction multiplier for N to compute the fraction of mineral N which will leach to the next layer when there is a saturated water flow; normal leaching is a function of sand content	fraction N	1	0.2	2	0.43
flig(1,1)c	Intercept for equation to predict lignin content fraction based on annual rainfall for aboveground material for corn	fraction of lignin	0.12	0.09	0.15	0.09
flig(1,1)s	Intercept for equation to predict lignin content fraction based on annual rainfall for aboveground material for soybean	fraction of lignin	0.12	0.09	0.15	0.09
fwloss(1)	Scaling factor for interception and evaporation of precipitation by live and standing dead biomass	unitless	1	0.2	2	1
fwloss(2)	Scaling factor for bare soil evaporation of precipitation (H_2O loss)	unitless	1	0.2	2	1
fwloss(3)	Scaling factor for transpiration water loss (H_2O loss)	unitless	1	0.2	2	1
fwloss(4)	Scaling factor for potential evapotranspiration	unitless	0.75	0.2	2	0.5
himax	Harvest index maximum for corn (fraction of aboveground live C in grain)	fraction of C	0.5	0.4	0.6	0.535
hiwsf	Harvest index water stress factor = 0 no effect of water stress = 1 no grain yield with maximum water stress for corn	fraction	0.6	0.000001	1	1
hours_rain	Duration of each rain event	hours	4	1	10	4.11
nit_amnt	Maximum daily nitrification amount	g N/m^2	0.4	0.1	4	1.91
nitrified_n	Proportion of nitrified N that is lost as N_2O (0.0−1.0)	fraction N	0.8	0.5	1	1
omlech(1)	Intercept for the effect of sand on leaching of organic compounds	unitless	0.03	0.000001	1	0.001
omlech(2)	Slope for the effect of sand on leaching of organic compounds	unitless	0.12	0.02	0.8	0.02
omlech(3)	The amount of water that needs to flow out of water layer 2 to leach organic C at the maximum rate	cm/day	1.9	0.02	2	2
pabres	Amount of residue which will give maximum direct absorption of N	g C m/^{2}	100	70	200	70

Parameter	Description	Units				
peftxa	Intercept parameter for regression equation to compute the effect of soil texture on the microbe decomposition rate (the effect of texture when there is no sand in the soil)	unitless	0.2	0.1	0.7	0.1
peftxb	Slope parameter for the regression equation to compute the effect of soil texture on the microbe decomposition rate; the slope is multiplied by the sand content fraction	unitless	0.4	0.2	1.5	0.2
ppdf(1)c	Optimum temperature for production for parameterization of a Poisson Density Function curve to simulate temperature effect on growth of corn	°C	30	27	33	32.71
ppdf(1)s	Optimum temperature for production for parameterization of a Poisson Density Function curve to simulate temperature effect on growth of soybean	°C	27	24	30	29.98
ppdf(2)c	Maximum temperature for production for parameterization of a Poisson Density Function curve to simulate temperature effect on growth of corn	°C	45	40	50	40
ppdf(2)s	Maximum temperature for production for parameterization of a Poisson Density Function curve to simulate temperature effect on growth of soybean	°C	40	35	45	35
prdx(1)c	Coefficient for calculating potential aboveground monthly production as a function of solar radiation outside the atmosphere for corn	g C/m^2/langleys of shortwave radiation	1.05	0.1	10	1.12
prdx(1)s	Coefficient for calculating potential aboveground monthly production as a function of solar radiation outside the atmosphere for soybean	g C/m^2/langleys of shortwave radiation	0.8	0.1	10	5.816
prdx_g3n(1)	Coefficient for calculating potential aboveground monthly production as a function of solar radiation outside the atmosphere for mixed grasses	g C/m^2/langleys of shortwave radiation	0.35	0.1	1.5	1.418
rces2(2,1)	Initial C/N ratio in soil organic matter with intermediate turnover (slow SOM)	C/N	16	5	20	20
rces3(1)	Initial C/N ratio in soil organic matter with slow turnover (passive SOM)	C/N	7	2	10	10
rcestr(1)	C/N ratio for structural material (fixed parameter value)	C/N	100	50	300	50
riint	Root impact intercept used by rtimp; used for calculating the impact of root biomass on nutrient availability	unitless	0.5	0.2	0.7	0.7
snfxmx(1)	Symbiotic N fixation maximum for soybean	g N/g C new growth	0.04	0.00001	1	0.003
teff(1)	"x" location of inflection point, for determining the temperature component of DEFAC, the decomposition factor	unitless	15.4	5	20	6.932
teff(2)	"y" location of inflection point, for determining the temperature component of DEFAC, the decomposition factor	unitless	11.75	2	20	2
teff(3)	Step size (distance from the maximum point to the minimum point), for determining the temperature component of DEFAC, the decomposition factor	unitless	29.7	10	40	10
teff(4)	Slope of line at inflection point, for determining the temperature component of DEFAC, the decomposition factor	unitless	0.031	0.01	0.04	0.04
varat11(1,1)	Maximum C/N ratio for material entering surface som1	C/N	15	12	17	17
varat11(2,1)	Minimum C/N ratio for material entering surface som1	C/N	6	4	6	6
varat12(1,1)	Maximum C/N ratio for material entering soil som1	C/N	14	11	17	17
varat12(2,1)	Minimum C/N ratio for material entering soil som1	C/N	3	2	4	4
water_temp	Min water/temperature limitation coefficient for nitrify	unitless	0.03	0.01	0.08	0.01

Identifiability analysis evaluates the degree to which parameters can be estimated uniquely (Doherty and Hunt, 2009) by relating the contributions made by the adjustable parameters to any of the eigenvectors spanning the calibration solution space. All eigenvectors are normalized; hence the largest contribution that any parameter can make to an eigenvector is 1.0. Parameters with low identifiability are inestimable because they have a large projection in the null space of the inversion problem, e.g., due to correlation with one or more other parameters or low sensitivity to all observations. Parameters with an identifiability of 1.0 are theoretically completely estimable because they lie entirely in the inversion solution space. This implies that the null space contribution to parameter estimation error is zero, and any mismatch between the measured and simulated values results not from the inversion problem, but from sources of systematic uncertainty such as measurement inaccuracy, imperfections in the conceptual model, and approximations made in formulating a numerical model to represent complex physical processes (Doherty and Hunt, 2010b). It should be noted that the identifiability statistic, based as it is on a linear approximation of nonlinear processes, a necessarily incomplete model, and imperfect measurements, is not a precise quantitative measure, but rather provides qualitative insights into relative parameter estimability (Doherty and Hunt, 2009). In the present study, parameters with identifiability >0.7 were considered to be identifiable with the available calibration dataset. Unlike sensitivity analysis, identifiability analysis accounts for parameter correlations that can make it impossible to uniquely estimate even highly sensitive parameters (Doherty and Hunt, 2010a).

Table 3
DayCent calibration and validation results for individual observation groups. Simulated values to field observation statistic was described using sum of weighted squared residuals (SWSR), absolute root mean square error (RMSE), relative root mean square error (rRMSE), index of agreement (d), mean bias (MB) and coefficient of determination (r^2).

		Calibration period (2011–2012)			Validation period (2013)		
		Observed values	Default model	Calibrated model	Observed values	Default model	Calibrated model
Crop Productivity	SWSR		10 000	102		24 936	10 581
	RMSE		106.27	10.75		205.53	133.88
	rRMSE		0.22	0.02		0.48	0.32
	d		0.97	1.00		0.67	0.78
	MB		9.42	−4.25		−201.30	−127.22
	Corn ANPP (g C m^{-2})	815.4	943.1	818.2	565.1	322.3	396.2
	Corn grain yield (g C m^{-2})	441.2	455.9	443.9	284.0	124.2	198.5
	Soybean grain yield (g C m^{-2})	196.7	47.1	178.5	–	–	–
Soil organic Carbon	SWSR		10 000	270	–	–	–
	RMSE		1370.5	225.3	–	–	–
	MB		−1370.5	−225.3	–	–	–
	SOC (g C m^{-2})	6147	4735	5922	–	4712	5928
Soil N$_2$O Emissions	SWSR		10 000	6084		2106	760
	RMSE		138.69	108.18		83.32	50.05
	rRMSE		2.04	1.59		1.62	0.97
	d		0.38	0.62		0.41	0.89
	MB		−57.44	−25.23		−33.21	20.50
	r^2		0.28	0.49		0.43	0.71
	Daily N$_2$O flux (g N ha^{-1})	112.40[a]	15.08[a]	51.42[a]	51.42	11.92	48.62
		5.28[b]	4.68[b]	19.53[b]			
	Annual N$_2$O flux (kg N ha^{-1})	16.53[a]	2.56[a]	8.74[a]	5.21	1.75	7.15
		1.08[b]	0.75[b]	3.12[b]			
Volumetric soil water Content	SWSR		10 000	1498		18 974	9832
	RMSE		0.06	0.02		0.11	0.08
	rRMSE		0.21	0.08		0.37	0.27
	d		0.83	0.96		0.70	0.77
	MB		−0.007	−0.003		−0.08	0.001
	r^2		0.73	0.86		0.51	0.47
	Mean VSWC (cm^3 cm^{-3})	0.30[a]	0.24[a]	0.30[a]	0.30	0.18	0.26
		0.29[b]	0.21[b]	0.26[b]			
Soil NO$_3^-$−N concentration	SWSR		10 000	7022		8990	9048
	RMSE		82.40	69.05		94.45	94.75
	rRMSE		1.69	1.41		1.25	1.25
	d		0.39	0.57		0.53	0.55
	MB		−32.67	4.09		−43.93	2.57
	r^2		0.08	0.29		0.73	0.19
	Mean NO$_3$−N (mg N kg^{-1})	64.37[a]	10.74[a]	58.13[a]	75.59	34.96	99.46
		5.32[b]	2.01[b]	14.36[b]			
Soil NH$_4^+$−N concentration	SWSR		10 000	10 073		7846	7980
	RMSE		278.98	279.99		282.59	284.99
	rRMSE		2.77	2.78		1.64	1.66
	d		0.34	0.35		0.44	0.44
	MB		−65.84	−62.34		−114.13	−121.63
	r^2		0.41	0.35		0.75	0.92
	Mean NH$_4$−N (mg N kg^{-1})	141.35[a]	35.32[a]	33.62[a]	171.84	54.92	37.77
		3.52[b]	5.41[b]	14.48[b]			
Soil Temperature	SWSR		10 000	5647		7394	6629
	RMSE		2.80	2.10		3.27	3.09
	rRMSE		0.14	0.10		0.16	0.15
	d		0.93	0.96		0.72	0.77
	MB		−1.01	−0.04		−0.76	−1.46
	r^2		0.80	0.86		0.51	0.47
	Mean soil temperature (°C)	19.54[a]	19.09[a]	20.23[a]	21.05	21.22	20.75
		20.84[b]	20.71[b]	20.75[b]			

[a] Values refer to 2011 calibration year.
[b] Values refer to year 2012.
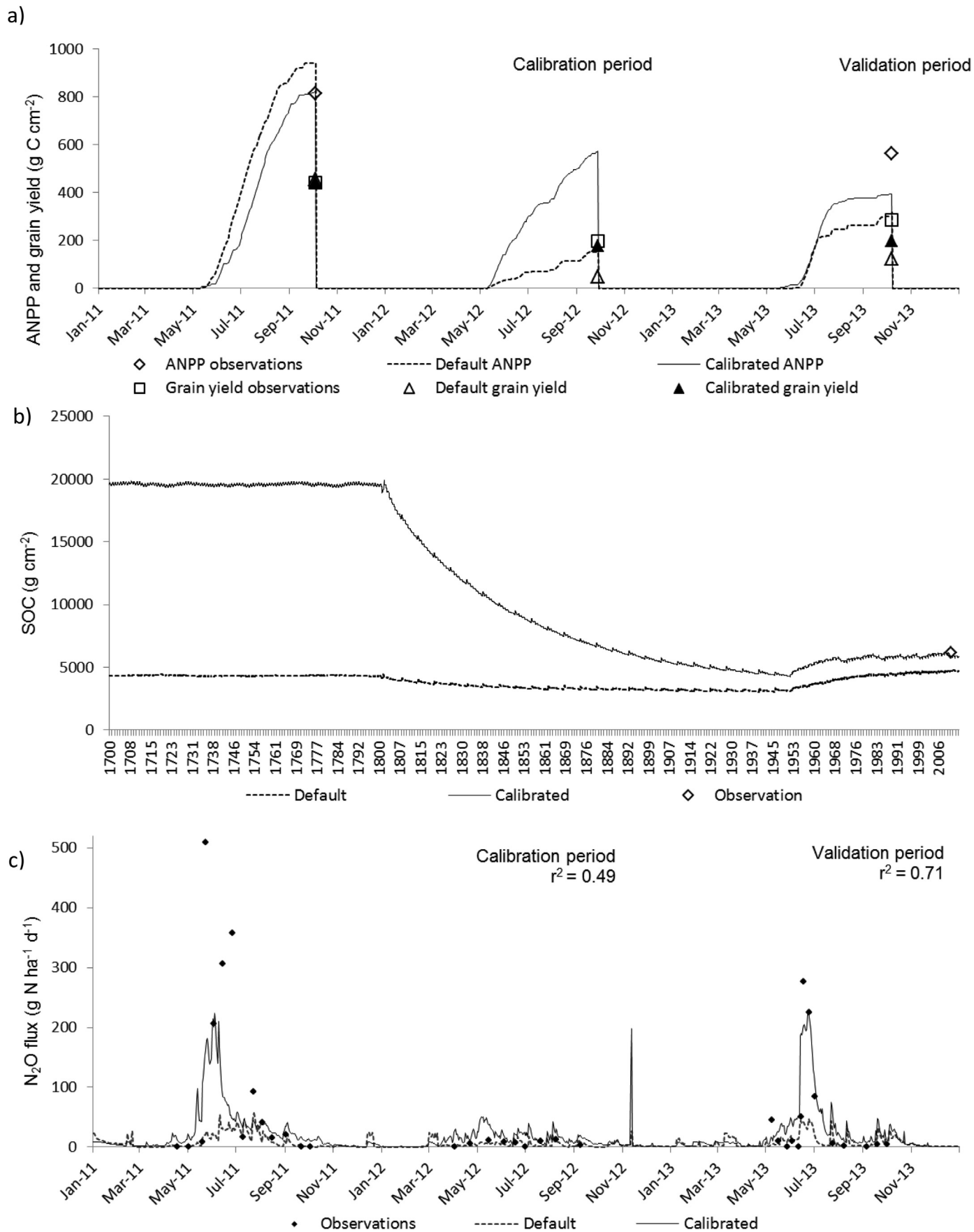
Fig. 2. DayCent simulated values and field observations: a) aboveground net primary productivity (ANPP) and grain yields (ANPP was not measured during soybean phase of the rotation), b) soil organic carbon (SOC), c) daily nitrous oxide (N_2O–N) fluxes, d) volumetric soil water content (VSWC) and e) soil temperature during calibration (2011−2012) and validation period (2013) and associated coefficient of determination (r^2).

d)

e)
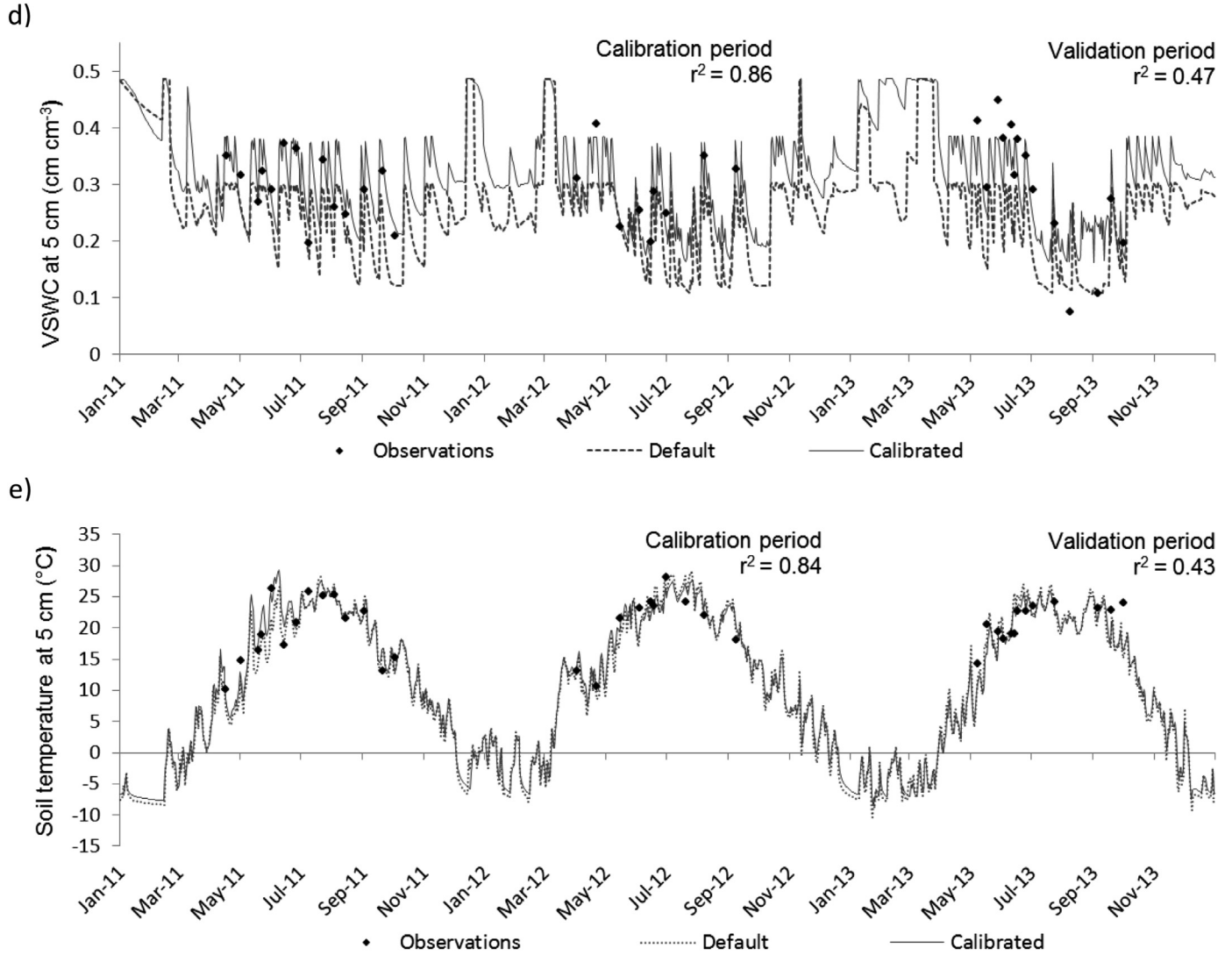
Fig. 2. (*continued*).

2.4. DayCent model validation

Calibration performance was quantified using multiple statistical criteria (Moriasi et al., 2007; Nolan et al., 2011; Wallach et al., 2014): absolute root mean square error (RMSE), relative root mean square error (rRMSE), sum of weighted squared residuals (SWSR), index of agreement (d), coefficient of determination (r^2) and mean bias (MB) as follows:

$$RMSE = \sqrt{\frac{1}{m} \sum_{i=1}^{m} (y_i - y'_i)^2}$$

$$rRMSE = \frac{\sqrt{\frac{1}{m} \sum_{i=1}^{m} (y_i - y'_i)^2}}{|\overline{y}|}$$

$$SWSR = \sum_{i=1}^{m} weighted \ (y_i - y'_i)^2$$

$$d = 1 - \frac{\sum_{i=1}^{m} (y_i - y'_i)^2}{\sum_{i=1}^{m} (|y'_i - \overline{y}| + |y_i - \overline{y}|)^2}$$

$$r^2 = 1 - \frac{\sum_{i=1}^{m} (y_i - y'_i)^2}{\sum_{i=1}^{m} (y_i - \overline{y})^2}$$

$$MB = \frac{1}{m} \sum_{i=1}^{m} (y'_i - y_i)$$

where y is observation, y' denotes the simulated value, $\overline{y}$ is the mean of the observations, m represents the number of observations, and subscript *i* denotes *i*th observation.

3. Results

3.1. DayCent calibration

DayCent was calibrated using two years of data (2011–2012). The final PEST run required 40 optimization iterations and 6004 DayCent model runs. The number of singular values used in SVD ranged from 11 to 57 on an iteration-by-iteration basis, based on a stability criterion. The total objective function (total SWSR) decreased by 56%. Model fit to crop productivity, SOC, soil N_2O, VSWC, temperature and NO_3^- was improved compared to the default simulation (Table 3); i.e., all these observation groups were reproduced by the calibrated model with lower rRMSE and higher d. The greatest improvement was observed in simulating crop productivity (Fig. 2a), where the SWSR was reduced by 99% and resulted in rRMSE of 0.02 and d of 1.0. The SOC SWSR was reduced

Table 4

DayCent parameter correlation structure. Strong correlations ($R^2 > 0.8$) are highlighted in red. Parameter definitions are in Table 2.

	ppdf(1)c	ppdf(2)c	ppdf(1)s	ppdf(2)s	dec4	dmpflux	aneref(3)	prdx(1)c	dec1(1)	dmp_st	teff(3)	snfxmx(1)	teff(4)	dec5(2)	teff(2)	fwloss(4)	prdx(1)s	flig(1,1)c	damrmn(1)	himax	favail(1)	epnfa(2)	fleach(3)
ppdf(1)c	1.00	0.83	-0.27	0.47	0.20	0.06	-0.30	-0.43	0.28	0.07	-0.62	-0.44	0.53	0.43	-0.61	0.25	-0.46	-0.21	0.21	-0.07	-0.44	-0.05	0.06
ppdf(2)c		1.00	-0.49	0.38	0.24	0.07	-0.35	-0.85	-0.11	0.00	-0.37	-0.58	0.35	0.75	-0.35	0.15	-0.25	-0.23	0.17	-0.12	-0.42	0.02	0.00
ppdf(1)s			1.00	0.39	-0.24	0.06	0.30	0.56	0.36	0.07	-0.36	-0.02	0.26	-0.43	-0.34	-0.18	-0.23	0.15	0.03	-0.10	0.22	-0.10	-0.14
ppdf(2)s				1.00	0.07	0.09	-0.05	-0.13	0.34	0.03	-0.85	-0.78	0.80	0.15	-0.88	0.02	-0.77	0.10	0.08	-0.06	-0.38	0.15	-0.03
dec4					1.00	0.02	-0.96	-0.14	-0.06	0.00	-0.07	-0.13	0.06	0.12	-0.06	0.07	-0.05	0.42	-0.10	0.37	-0.44	0.61	-0.08
dmpflux						1.00	-0.03	-0.08	0.13	-0.01	-0.05	0.02	0.04	0.07	-0.09	-0.37	-0.17	-0.03	0.05	-0.22	-0.10	-0.01	0.00
aneref(3)							1.00	0.24	0.06	0.01	0.08	0.16	-0.08	-0.21	0.07	-0.10	0.06	-0.28	0.07	-0.30	0.44	-0.50	0.05
prdx(1)c								1.00	0.42	0.06	0.00	0.48	-0.06	-0.83	-0.01	0.03	-0.01	0.25	-0.11	0.17	0.21	-0.01	0.03
dec1(1)									1.00	0.09	-0.55	0.19	0.51	-0.28	-0.66	-0.21	-0.68	-0.02	0.12	-0.07	-0.19	-0.19	0.08
dmp_st										1.00	-0.06	0.02	0.10	0.04	-0.07	0.06	0.00	0.04	0.02	0.01	-0.04	0.00	-0.02
teff(3)											1.00	0.64	-0.91	-0.06	0.96	-0.15	0.66	-0.02	-0.11	0.03	0.33	-0.01	-0.11
snfxmx(1)												1.00	-0.66	-0.40	0.58	-0.26	0.33	0.00	-0.04	0.04	0.30	-0.18	-0.02
teff(4)													1.00	0.03	-0.92	0.13	-0.63	0.00	0.09	-0.04	-0.32	0.01	0.11
dec5(2)														1.00	-0.04	0.00	0.00	-0.19	0.11	-0.14	-0.21	0.00	-0.04
teff(2)															1.00	-0.05	0.80	-0.01	-0.13	0.05	0.38	0.00	-0.08
fwloss(4)																1.00	0.21	-0.06	0.01	0.21	-0.01	0.03	0.05
prdx(1)s																	1.00	0.03	-0.14	0.10	0.38	0.02	0.00
flig(1,1)c																		1.00	-0.05	0.33	-0.07	0.90	0.08
damrmn(1)																			1.00	-0.18	-0.01	-0.07	-0.12
himax																				1.00	-0.13	0.42	0.03
favail(1)																					1.00	-0.15	0.04
epnfa(2)																						1.00	0.08
fleach(3)																							1.00

	dec3(2)	riint	epnfs(2)	varat11(2,1)	flig_s(1,1)	epnfs(1)	peftxa	omlech(1)	rcestr(1)	varat12(2,1)	water_temp	varat12(1,1)	teff(1)	nit_amnt	cfrtcw(2)	peftxb	dec2(2)	dec3(1)	rces2(2,1)	varat11(1,1)	dec2(1)	damr(2,1)
ppdf(1)c	-0.05	-0.37	-0.22	0.26	0.10	-0.20	-0.03	-0.08	-0.25	0.11	-0.25	0.32	-0.35	0.19	-0.13	0.13	0.27	0.32	-0.05	0.36	-0.61	0.03
ppdf(2)c	-0.07	-0.14	-0.27	0.07	0.12	-0.21	0.00	-0.12	-0.17	0.21	-0.25	0.31	-0.36	0.10	-0.14	0.11	0.30	0.24	-0.11	0.27	-0.52	0.10
ppdf(1)s	-0.12	0.11	0.01	0.39	-0.09	-0.04	0.08	0.01	-0.17	-0.57	0.04	-0.11	-0.32	0.02	-0.04	-0.01	-0.11	-0.05	0.22	0.02	-0.29	0.05
ppdf(2)s	0.00	-0.26	-0.11	0.63	-0.16	-0.02	0.02	-0.23	-0.20	0.12	-0.18	0.00	-0.91	0.08	0.07	-0.04	0.29	-0.02	0.50	-0.75	0.28	
dec4	0.54	-0.24	0.23	0.18	-0.46	0.44	-0.28	-0.47	-0.12	0.16	0.05	-0.38	-0.06	-0.39	0.73	-0.15	0.89	0.11	-0.26	0.37	-0.05	0.03
Dmpflux	0.00	-0.26	-0.01	-0.02	0.03	-0.01	0.01	0.00	0.00	0.04	-0.03	0.06	-0.04	0.03	-0.01	0.00	0.03	0.04	-0.02	0.03	-0.09	-0.02
aneref(3)	-0.48	0.26	-0.16	-0.13	0.33	-0.33	0.28	0.34	0.20	-0.07	0.00	0.24	0.03	0.28	-0.53	0.06	-0.84	-0.25	0.26	-0.34	0.12	0.07
prdx(1)c	0.11	-0.09	0.26	0.22	-0.17	0.20	-0.04	0.05	0.03	-0.21	0.18	-0.28	0.21	-0.03	0.18	-0.08	-0.18	-0.13	0.11	-0.03	0.27	-0.05
dec1(1)	0.00	-0.64	0.08	0.39	0.02	-0.03	-0.01	0.06	-0.17	-0.21	-0.08	0.14	-0.12	0.22	-0.05	0.03	-0.02	0.26	0.09	0.27	-0.33	-0.15
dmp_st	-0.01	-0.03	0.00	0.11	-0.04	0.00	0.00	-0.03	-0.04	-0.07	-0.01	-0.01	-0.01	-0.05	0.01	0.00	0.03	0.02	0.01	0.07	-0.11	0.05
teff(3)	-0.02	0.26	0.06	-0.65	0.08	0.04	0.02	0.11	0.27	0.05	0.19	-0.11	0.74	-0.21	0.01	-0.02	-0.23	-0.15	-0.06	-0.48	0.75	-0.09
snfxmx(1)	0.01	-0.07	0.17	-0.39	0.08	0.05	-0.02	0.21	0.14	-0.24	0.19	-0.06	0.85	-0.06	-0.01	0.02	-0.31	0.04	0.02	-0.35	0.66	-0.23
teff(4)	0.02	-0.26	-0.05	0.61	-0.05	-0.04	-0.02	-0.09	-0.23	-0.01	-0.20	0.13	-0.81	0.22	-0.02	0.02	0.22	0.15	0.06	0.46	-0.77	0.04
dec5(2)	-0.10	0.03	-0.23	-0.13	0.11	-0.18	0.04	-0.06	-0.06	0.14	-0.16	0.25	-0.14	0.02	-0.15	0.07	0.17	0.13	-0.09	0.06	-0.23	0.08
teff(2)	-0.01	0.42	0.06	-0.65	0.07	0.05	0.01	0.11	0.25	0.01	0.20	-0.13	0.76	-0.21	0.00	-0.02	-0.23	-0.16	-0.06	-0.50	0.74	-0.08
fwloss(4)	0.01	0.20	-0.06	0.04	0.03	-0.04	-0.04	-0.03	-0.07	0.07	-0.04	0.04	-0.09	0.05	-0.02	0.05	0.07	0.03	0.00	0.03	-0.06	0.00
prdx(1)s	0.00	0.67	0.07	-0.43	0.01	0.06	0.00	0.10	0.16	-0.11	0.17	-0.14	0.56	-0.16	0.00	-0.02	-0.17	-0.16	-0.02	-0.40	0.57	-0.03
flig(1,1)c	0.56	0.02	0.35	0.21	-0.99	0.69	-0.21	-0.27	0.57	0.24	0.09	-0.98	-0.13	-0.44	0.61	-0.36	0.53	-0.70	-0.14	0.15	0.10	0.00
damrmn(1)	-0.19	-0.12	-0.30	-0.03	0.03	-0.23	0.07	0.00	-0.02	-0.19	-0.06	0.09	-0.03	0.00	-0.21	0.10	0.00	0.03	0.16	-0.03	-0.17	-0.05
Himax	0.57	0.01	0.25	0.13	-0.32	0.37	-0.59	0.15	0.21	0.23	0.08	-0.34	0.04	-0.31	0.52	0.29	0.22	-0.23	-0.13	0.17	0.18	0.00
favail(1)	-0.27	0.46	-0.06	-0.72	0.13	-0.11	0.18	0.40	0.45	-0.32	0.03	0.01	0.31	-0.04	-0.30	-0.03	-0.36	-0.36	0.11	-0.95	0.26	-0.49
epnfa(2)	0.61	-0.04	0.30	0.10	-0.92	0.68	-0.26	-0.28	0.57	0.42	-0.01	-0.89	-0.19	-0.53	0.67	-0.32	0.72	-0.69	-0.20	0.15	0.05	0.04
fleach(3)	0.16	-0.08	0.25	-0.02	-0.09	0.21	-0.03	0.16	0.26	0.13	-0.08	-0.07	0.03	0.38	-0.10	-0.14	-0.05	-0.13	0.01	-0.04	-0.15	-0.15
dec3(2)	1.00	-0.14	0.73	0.19	-0.57	0.84	-0.80	-0.21	0.27	0.25	0.13	-0.55	-0.01	-0.31	0.55	0.12	0.45	-0.25	-0.18	0.28	0.10	-0.16
Riint		1.00	-0.07	-0.16	0.02	-0.07	0.07	0.07	0.05	-0.24	0.12	-0.10	0.04	-0.04	-0.10	0.02	-0.21	-0.22	0.09	-0.33	0.20	0.11
epnfs(2)			1.00	0.10	-0.32	0.90	-0.33	-0.13	0.19	0.14	0.29	-0.35	0.10	-0.22	0.37	-0.33	0.14	-0.17	-0.08	0.11	0.18	-0.19
varat11(2,1)				1.00	-0.23	0.12	-0.13	-0.35	-0.47	0.01	0.01	-0.14	-0.59	0.10	0.26	0.00	0.22	0.20	0.05	0.90	-0.43	0.52
flig(1,1)s					1.00	-0.68	0.22	0.29	-0.56	-0.28	-0.06	0.96	0.17	0.43	-0.61	0.35	-0.58	0.68	0.16	-0.20	-0.04	-0.01
epnfs(1)						1.00	-0.38	-0.22	0.42	0.30	0.23	-0.68	0.00	-0.40	0.58	-0.39	0.42	-0.45	-0.14	0.15	0.17	-0.15
Peftxa							1.00	0.00	-0.10	-0.07	-0.06	0.20	-0.03	0.13	-0.22	-0.69	-0.16	0.06	0.10	-0.19	-0.04	0.17
omlech(1)								1.00	0.24	-0.21	-0.06	0.26	0.24	0.21	-0.52	0.22	-0.57	-0.04	0.11	-0.41	0.06	-0.48
rcestr(1)									1.00	0.35	-0.09	-0.59	0.15	-0.29	0.13	-0.21	0.00	-0.87	0.01	-0.49	0.27	-0.32
varat12(2,1)										1.00	0.04	-0.27	-0.15	-0.18	0.35	-0.19	0.17	-0.40	-0.25	0.22	0.19	0.35
water_temp											1.00	-0.13	0.16	-0.08	0.20	-0.06	-0.04	0.04	-0.06	0.00	0.25	-0.16
varat12(1,1)												1.00	0.04	0.44	-0.61	0.36	-0.47	0.73	0.15	-0.09	-0.24	-0.02
teff(1)													1.00	-0.04	-0.09	0.06	-0.29	0.10	-0.03	-0.45	0.72	-0.30
nit_amnt														1.00	-0.49	0.18	-0.36	0.40	0.15	0.04	-0.26	-0.16
cfrtcw(2)															1.00	-0.27	0.67	-0.27	-0.22	0.33	0.18	0.23
peftxb																1.00	-0.24	0.28	0.04	0.02	-0.07	-0.08
dec2(2)																	1.00	-0.11	-0.19	0.33	-0.22	0.08
dec3(1)																		1.00	0.01	0.30	-0.21	-0.01
rces2(2,1)																			1.00	-0.05	-0.09	-0.01
varat11(1,1)																				1.00	-0.32	0.55
dec2(1)																					1.00	-0.02
damr(2,1)																						1.00

by 97% (Fig. 2b). Simulated VSWC at 5 cm depth closely matched the seasonal dynamic and magnitude of the observations (Fig. 2d), as did soil temperature at 5 cm depth (Fig. 2e). Daily N_2O fluxes were underestimated during the first year of the calibration period (corn phase) and slightly overestimated during the second year (soybean phase). Over both years, N_2O daily fluxes were underestimated by 37% (Fig. 2c), although the dynamics of the daily fluxes, mainly driven by the fertilizer application, were reproduced satisfactorily. Fit of simulated to observed N_2O flux was improved, reducing SWSR by 39%. Nevertheless, the calibrated model failed to reproduce the magnitude of an N_2O flux peak that followed the fertilization event in May 2011, increasing rRSME and reducing d. Similar performance was observed for soil NO_3^- at 10 cm depth; inverse modeling reduced the SWSR by 30% (Table 3). DayCent failed to reproduce the magnitude of the spike following the May 2011 fertilization event. Nevertheless, overall soil NO_3^- content was overestimated by 8.4%. PEST did not improve model fit to soil NH_4^+ relative to the default simulation. Simulated soil NH_4^+ was underestimated during the corn phase, mainly after fertilization, and slightly overestimated during the soybean phase, as were N_2O and NO_3^-. Over both years of the calibration period, soil NH_4^+ was underestimated by 62% (Table 3).

3.2. Estimated parameter values and parameter correlations

Estimated parameter values obtained through inverse modeling are shown in Table 2. Through the SVD-based regularization process, PEST changed values of 63 of the 67 parameters available for adjustment. The parameters values changed the most were: *dmpflux*, *dec4*, *epnfs(2)*, *epnfa(2)*, *prdx(1)s*, *nit_amnt*, *prdx_g3n(1)*, *fleach(2)*. Adjustment of 46 of the parameters was limited by their upper or lower bounds. Parameters that were not adjusted through the regularization and inverse process were those that scale the interception and evaporation of precipitation by live and standing dead biomass; the evaporation of precipitation from bare soil; transpiration water loss (*fwloss(1)*, *fwloss(2)*, *fwloss(3)*); and minimum C/N ratio for biomass entering active surface SOM (*varat11(2,1)*).

Adjusting *ppdf(1)c*, and *ppdf(2)c* narrowed the Poisson density function curve used in DayCent to describe the effect of temperature on corn growth, limiting corn growth to air temperatures between 24.5 and 40 °C. Similarly, adjusting *ppdf(1)s*, and *ppdf(2)s* narrowed the Poisson density function soybean growth curve, limiting soybean growth to air temperatures between 23.5 and 35 °C. These adjustments intensified crop growth within a narrowed temperature range, which inevitably led to higher sensitivity of crop growth to air temperature within this range. Reducing *snfxmx(1)* reduced the soybean maximum N fixation. Adjustments to *varat11(1,1)*, *varat12(1,1)* and *varat12(2,1)* resulted in substantial growth of the active SOM pool, particularly belowground. Altering of *teff(1)*, *teff(2)*, *teff(3)*, *teff(4)*, limited the decomposition curve such that there was no decomposition below ~1.5 °C, but rapid decomposition at higher temperatures. Modifications to *nit_amnt* and *nitrified_n* increased the maximum daily nitrification to 1.9 g N m^{-2} and changed the proportion of nitrified N lost as N_2O to 100%, respectively. Tuning of *dumpflux* resulted in slower water movement through the soil profile. Adjustment of *dmp_st* (the damping factor for calculating soil temperature by layer) resulted in slightly lower soil temperature, and changes in *floss(4)* led to lower evapotranspiration rates.

Examination of the correlation coefficient matrix for highly correlated parameters identified 15 parameter correlations with absolute value of correlation coefficient $|r| \geq 0.8$ and <0.9, and 13 correlations with $|r| \geq 0.9$ (Table 4). The correlations between *dec4* and *aneref(3)* (−0.96), *teff(2)* and *teff(3)* (0.96), *flig(1,1)c* and *flig(1,1)s* (−0.99), *flig(1,1)c* and *varat12(1,1)* (−0.98), and between *flig(1,1)s*

and *varat12(1,1)* (0.96), all had correlation coefficients greater than 0.95 (r > 0.95).

3.3. Parameter sensitivities and identifiability

The parameters most sensitive to crop productivity were those that define the Poisson density function curve describing the effect of temperature on corn growth (i.e., the optimum and maximum temperature for production, *ppdf(1)c* and *ppdf(2)c*), and a scaling factor of potential evapotranspiration (*fwloss(4)*) (Fig. 3a). The effect of the other parameters on crop productivity was minor. The most sensitive parameters to SOC were the parameters that determine the effect of temperature on decomposition rates (*teff(3)*, *teff(1)*, *teff(2)*, *teff(4)*), the maximum decomposition rate of SOM with slow and intermediate turnover (*dec4*, *dec5(2)*), the effect of temperature on soybean growth (*ppdf(1)s*, *ppdf(2)s*), the damping factor of soil temperature (*dmp_st*), and the maximum symbiotic N fixation by soybean (*snfxmx(1)*) (Fig. 3b).

The N_2O fluxes were calibrated by parameter changes enhancing nitrification more than denitrification. Parameters sensitive to soil N_2O emissions (resulting from nitrification and denitrification), were parameters that control the damping factor of soil temperature (*dmp_st*), the temperature effect on SOM decomposition (*teff(3)*, *teff(2)*, *teff(4)*, *teff(1)*) and crop growth (*ppdf(1)c*, *ppdf(1)s*, *ppdf(2)s*), the C/N ratio of decomposing biomass entering surface SOM (*varat11(1,1)*, *varat11(2,1)*), maximum daily nitrification (*nit_amnt*), N availability to plants (*favail(1)*), and potential evapotranspiration (*fwloss(4)*) (Fig. 3c). The N_2O observations contained sufficient information to identify four parameters, i.e., *fwloss(4)*, *nit_amnt*, *nitfied_n*, *dmp_st*; their identifiability was consistent with their relatively high sensitivity (Fig. 4a).

Parameters sensitive to VSWC were those governing the calculation of soil water content and potential evapotranspiration (i.e., *dmpflux*, *fwloss(4)*) and also those that describe the temperature effect on crop growth, maximum symbiotic N fixation (*ppdf(1)c*, *ppdf(2)c*, *ppdf(1)s*, *ppdf(2)s*, *snfxmx(1)*) and the temperature effect on SOM decomposition (*teff(3)*, *teff(2)*, *teff(4)*, *teff(1)*) (Fig. 3d). The VSWC observations possessed information essential for identification of six parameters, i.e., *fwloss(4)*, *dmpflux*, *prdx(1)c*, *ppdf(1)c*, *ppdf(1)s*, and *prdx(1)s*. Identifiability results were similar to sensitivity analysis results except that parameters *ppdf(2)c*, *ppdf(2)s*, *teff(3)*, *snfxmx(1)*, *teff(2)*, *eff(4)*, and *teff(1)* were highly sensitive, but were not identifiable through VSWC observations (Fig. 4b).

The most sensitive parameters to soil NO_3^- were parameters describing the temperature effect on crop growth (*ppdf(1)c*, *ppdf(2)c*, *ppdf(2)s*, *ppdf(1)s*); maximum daily nitrification (*nit_amnt*); N available to plants (*favail(1)*); the temperature effect on SOM decomposition (*teff(3)*, *teff(2)*, *teff(1)*, *teff(4)*); the C/N ratio of decomposing biomass entering surface SOM (*varat11(1,1)*, *varat11(2,1)*); fraction of mineral N that is leached to the next soil layer through saturated water flow (*fleach(1)*); the damping factor of soil temperature (*dmp_st*), and potential evapotranspiration (*fwloss(4)*; Fig. 3e). Fig. 4c shows that NO_3^- observations contained information for identifiability of two parameters (*fwloss(4)* and *nit_amnt*) and another two parameters were very near the threshold of identifiability (*fleach(3)* and *ppdf(1)c*).

Reflecting the close relationship between NO_3^- and NH_4^+ in soil processes, their sensitivity results were similar (Fig. 3f). Parameters highly sensitive to soil NH_4^+ were those describing the temperature effect on SOM decomposition (*teff(3)*, *teff(2)*, *teff(1)*, *teff(4)*) and crop growth (*ppdf(1)c*, *ppdf(2)c*, *ppdf(2)s*, *ppdf(1)s*), the damping factor of soil temperature (*dmp_st*), C/N ratio of decomposing biomass entering active SOM (*varat11(2,1)*, *varat11(1,1)*, *varat12(2,1)*), maximum daily nitrification (*nit_amnt*), maximum rate of surface metabolic decomposition and surface active organic
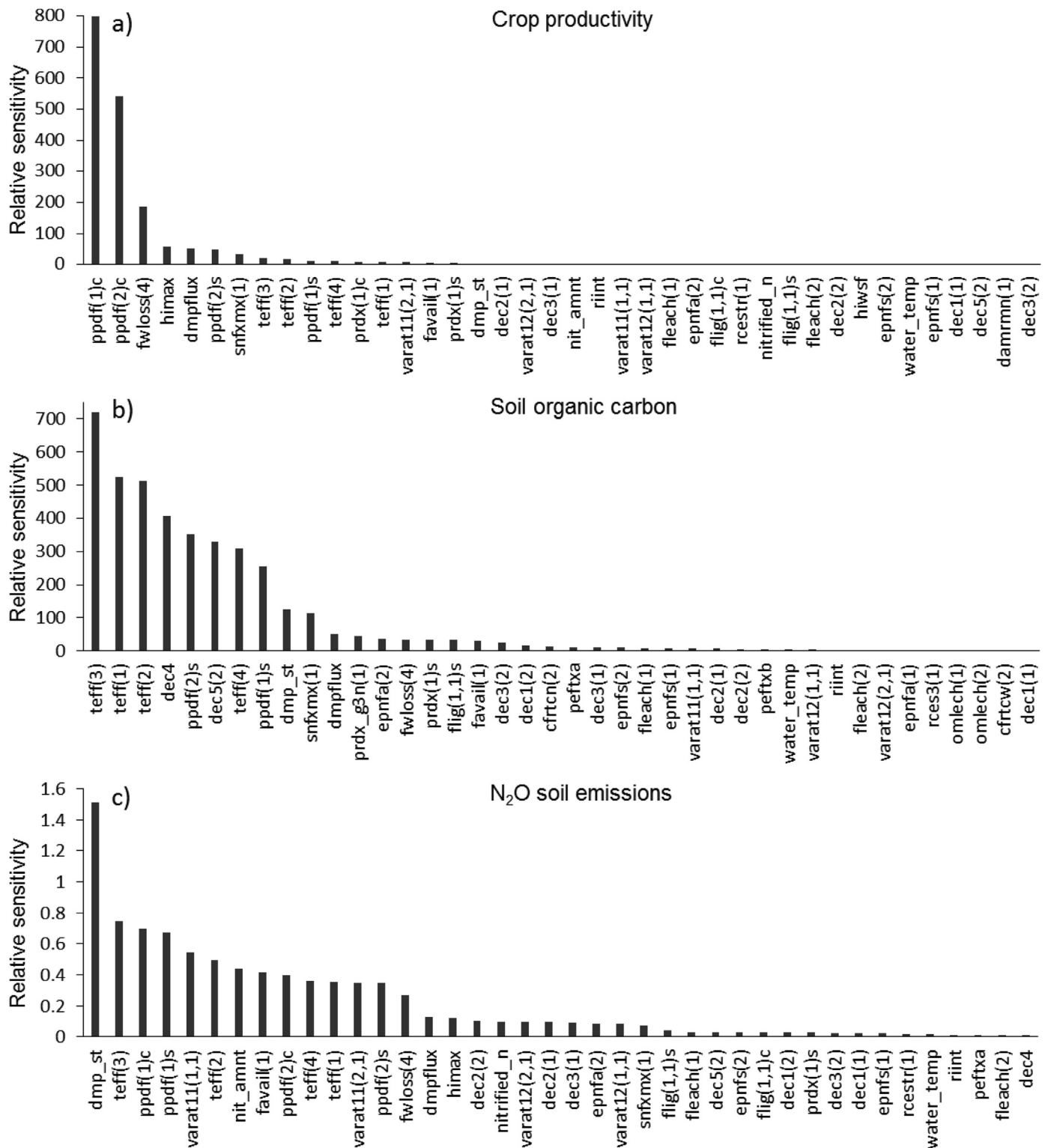
Fig. 3. Bar plot of DayCent relative composite parameter sensitivities to individual observation groups and to the entire calibration dataset based on their initial values. Parameter definitions are shown in Table 2.

matter (*dec2(1)*, *dec3(1)*), and N availability to crops (*favail(1)*). Analysis of identifiability through soil NH_4^+ yielded slightly different results than NO_3^- (Fig. 4d), i.e., only *fwloss(4)* was identifiable through NH_4^+ observations, while *ppdf(1)c* was just below the identifiability threshold.

As expected, the most sensitive parameter to soil temperature was *dmp_st*, followed by parameters *teff(3)*, *ppdf(2)s*, *teff(1)*, *ppdf(2)c*, *teff(2)*, *teff(4)*, *snfxmx(1)*, *epnfa(2)* (Fig. 3g). Some of which were previously mentioned for their effect on crop productivity and SOM decomposition. The last, *epnfa(2)*, influences wet and dry N
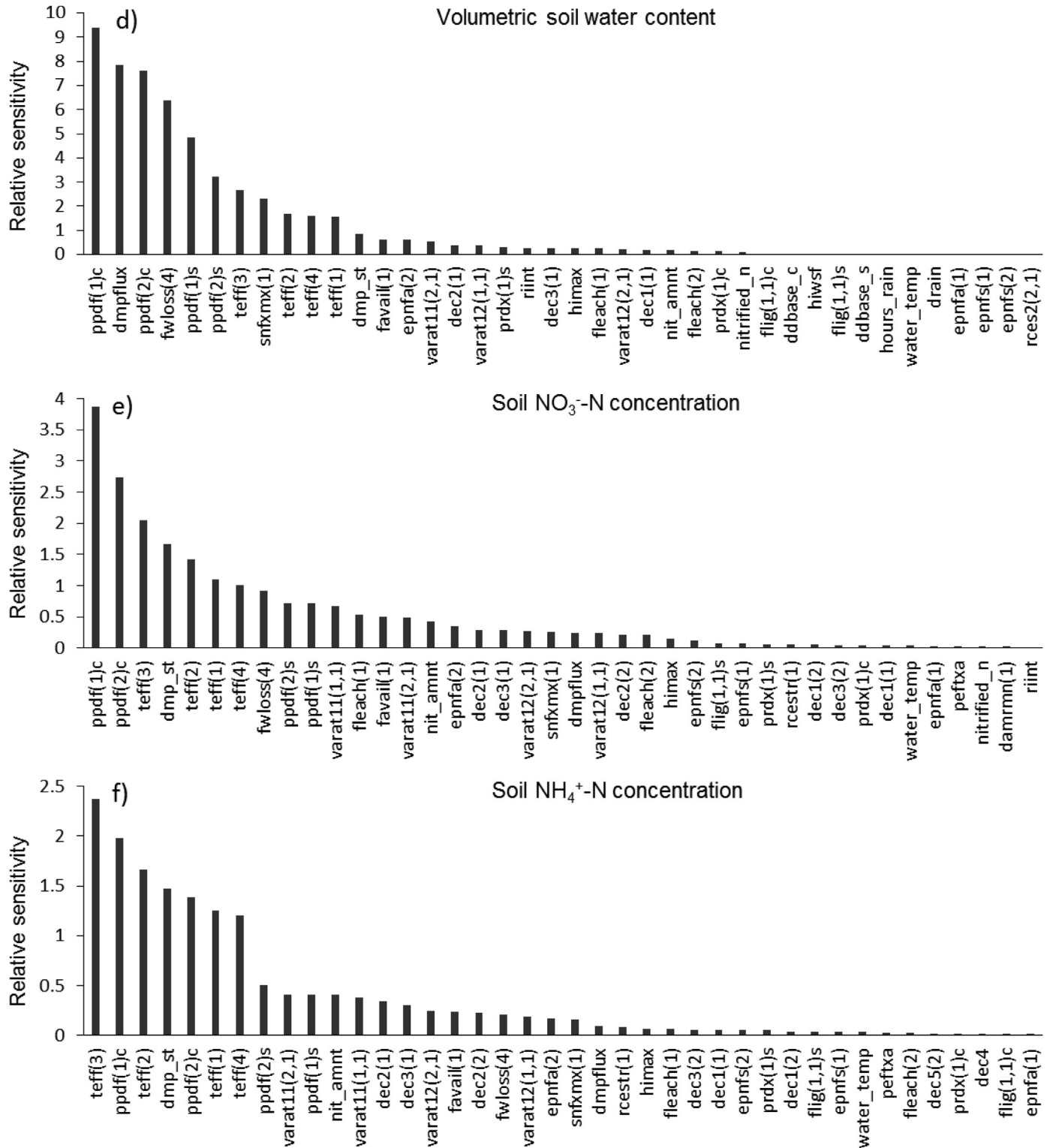
Fig. 3. (continued).

deposition. Identifiability analysis indicated that *dum_s_temp, fwloss(4), fleach(1)* and *prdx(1)s* were identifiable with soil temperature observations and *teff(3), teff(2), teff(1),teff(4), dec5(2), himax, prdx(1)c* approached the identifiability threshold (Fig. 4e).

Overall, the most sensitive parameters were *ppdf(1)c, ppdf(2)c, teff(3), fwloss(4), teff(1), teff(2), dmp_st, dec4, ppdf(2)s,dec5(2), teff(4), ppdf(1)s, dmpflux* (Fig. 3h). Information contained in the full calibration dataset including all observation groups, was sufficient to identify 16 parameters. Parameters such as *ppdf(2)c, teff(1), dec4, ppdf(2)s,dec5(2)* were not identifiable despite having substantial sensitivity (Fig. 4f). The sensitivity analysis was used as a diagnostic of the inverse process, not as a standalone analysis. For this reason this study does not present results on global sensitivity analysis or variation of parameter sensitivities with different assumptions.

g) Soil temperature
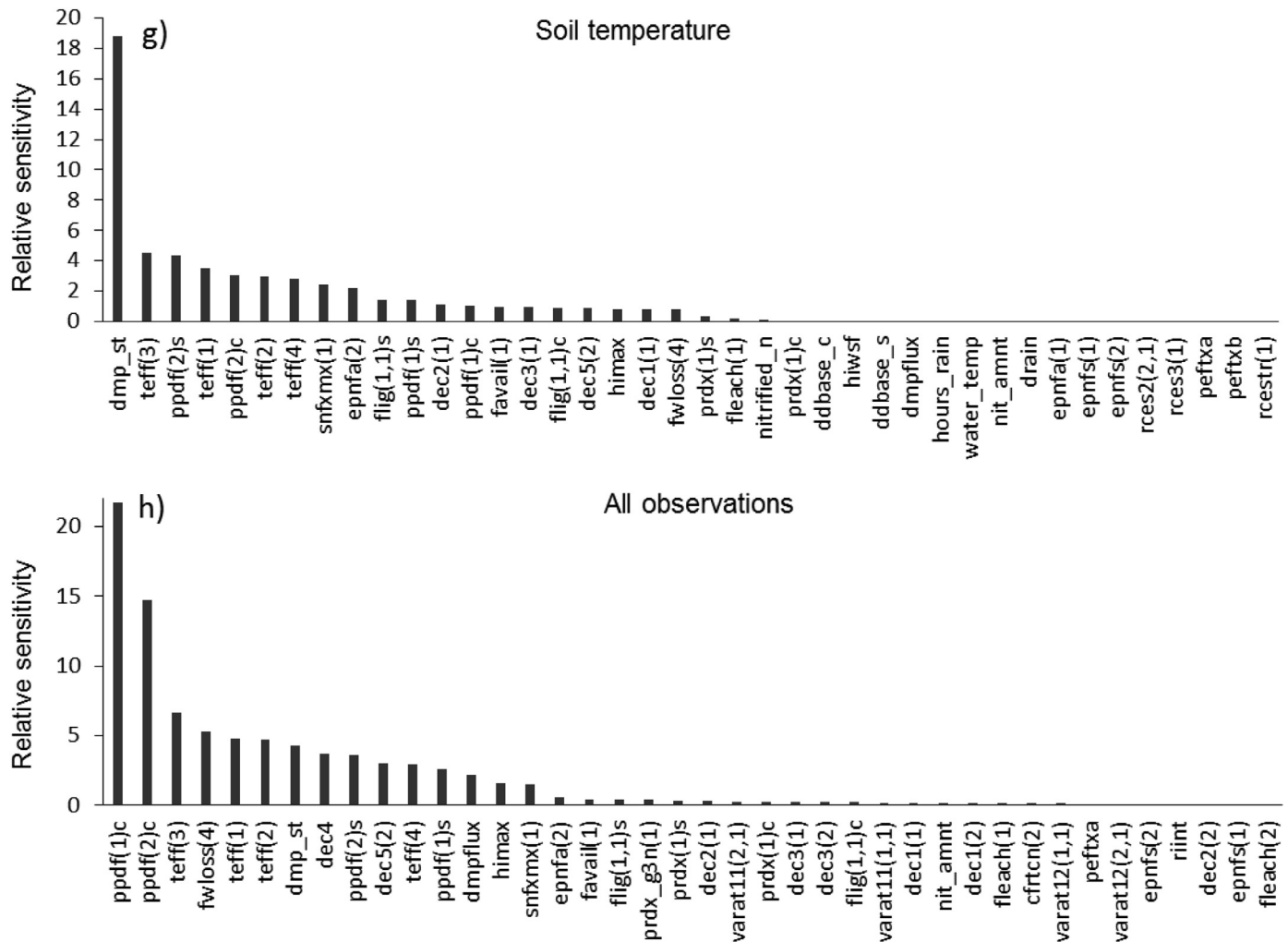
h) All observations

Fig. 3. (*continued*).

3.4. DayCent validation

The calibration was evaluated by comparing simulated outputs with a set of independent observations made in 2013 (i.e., the held-out "validation dataset"). Both the default model and the calibrated model were evaluated against this independent validation dataset. Model performance over the validation period was similar to that of the calibration period; crop productivity, soil N_2O, VSWC and temperature were reproduced with lower rRMSE and higher d compared to the default simulation (Table 3). The greatest improvement was observed in simulation of daily soil N_2O emissions, for which the SWSR was reduced by 64% with rRMSE of 0.97 and d of 0.89. This is a more accurate reproduction of N_2O than in the calibration period. The calibrated DayCent model failed to reproduce the magnitude of the N_2O spike observed after fertilization in May 2013 (Fig. 2c). Simulated daily fluxes on other dates were slightly overestimated (Table 3), and as a result, the simulated cumulative flux overestimated observed cumulative flux by 2 kg N ha^{-1} (Fig. 5). The simulation underestimated ANPP and grain yield by 30% (Fig. 2a). Simulation of VSWC was considerably improved compared to the default simulation as indicated by reduction of SWSR by 48% (Fig. 2d), however the dynamics were not reproduced as well as in the calibration period. Soil temperature was simulated satisfactorily.

Although inverse modeling improved simulation of all above mentioned observation groups compared with the default simulation during the validation period, it did not improve reproduction of soil NO_3^- and NH_4^+. The rRMSE and d of soil NO_3^- and NH_4^+ were unchanged by calibration (Table 3). The largest discrepancy between simulated and observed values was seen after fertilizer application. Considering all observation dates, soil NO_3^- was overestimated by 3.4% and soil NH_4^+ was underestimated by 71% (Table 3).

4. Discussion

4.1. DayCent calibration and validation

Our work demonstrates that inverse modeling can be used to calibrate several components of complex biogeochemical models simultaneously. In addition, inverse modeling provided valuable insights into model function through parameter sensitivities, identifiability and model correlation structure. As representations of our understanding of how a system functions, models are hypotheses that should to be tested. Inverse modeling is a powerful tool for doing this. It systematically interrogates the model, revealing relationships that are not otherwise obvious to model users or even developers.
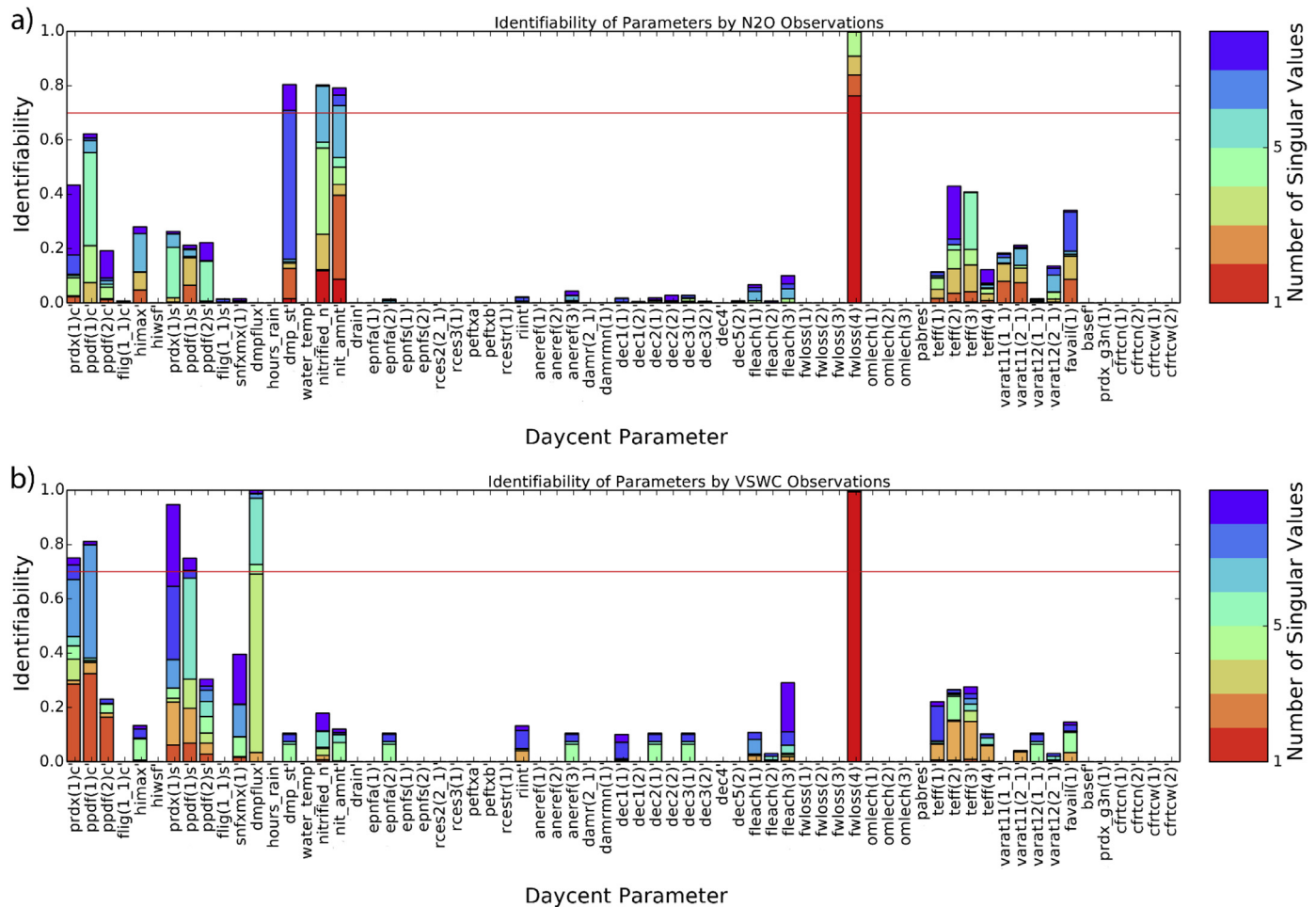
Fig. 4. Bar plot of DayCent parameter identifiability at the beginning of the inverse modeling by selected observation groups: a) soil N₂O emissions, b) volumetric soil water content, c) soil NO₃⁻−N concentration, d) soil NH₄⁺−N concentration, e) soil temperature and f) complete calibration dataset, with the contribution from each solution space eigenvector demarcated by color within each parameter-specific bar. All eigenvectors are normalized and arranged in order of decreasing singular value; therefore lower-numbered eigenvectors correspond to parameter combinations of greater identifiability. Red line represents a 0.7 threshold of parameter identifiability. Parameters with identifiability >0.7 and warmer colors may be qualitatively the most important process parameters. (For interpretation of the references to colour in this figure legend, the reader is referred to the web version of this article.)

Inverse modeling improved model performance in simulating crop productivity, SOC, VSWC, soil temperature and N₂O compared to the default simulation for both the calibration and validation datasets, however, it did not improve fit to soil NO₃⁻ and NH₄⁺ observations. Poor model fit can result from the model inversion improving the fit to one observation type at the expense of the fit to other observation types. In this study, we adopted an inter-group weighting strategy that equalized contributions made by different observation groups to the overall objective function to overcome differences in the number of field observations among groups, units of measure, and model structural uncertainty that is not considered in measurement error. Nonetheless, as the inversion algorithm progresses, groups trade off at the expense of one another. Another possible cause of the lack of improvement in soil NO₃⁻ and NH₄⁺ fit is a model parameterization in which the estimated parameters have very little sensitivity to the simulated values that were poorly fit. To investigate this, we examined the Jacobian matrix (elements of which express the sensitivity of simulated values for which there is a corresponding field observation to each adjustable parameter) and found substantial sensitivity of parameters to all available NH₄⁺ observations.

The remaining explanations for the poor fit to soil NO₃⁻ and NH₄⁺ are that the parameter bounds were too restrictive or the

model structure simply does not allow accurate simulation of the observed phenomenon. To explore these possibilities, we repeated the inverse modeling targeting only soil N observations (i.e., other observation groups were given zero weight). Even with the objective to match only the soil N observations, the SWSR for NH₄⁺ and NO₃⁻ were not reduced by more than 4% and 34%, respectively. Thus, the inability of the inverse modeling algorithm to improve simulation of soil N is probably the result of excessively restrictive parameter constraints, or by a structural error that limits the ability of DayCent to represent highly fertilized systems (i.e. structural noise; Doherty and Welter, 2010). The parameter constraints were informed by the code developers and the restriction of performance in this case may motivate reevaluation of the bounds.

Underestimation of ANPP during the validation period, despite accurate reproduction of soil temperature and VSWC dynamics, is further evidence that the DayCent representations of soil biochemistry are not completely correct (Del Grosso et al., 2008b; Parton et al., 2010). Calibrated DayCent also underestimated the magnitude of soil NO₃⁻ and NH₄⁺ following fertilization events, and since N₂O fluxes are strongly influenced by soil N, the magnitude of N₂O fluxes was underestimated as well. However, the dynamics of soil N and N₂O fluxes, which were significantly driven by fertilizer application, were represented reasonably well. The
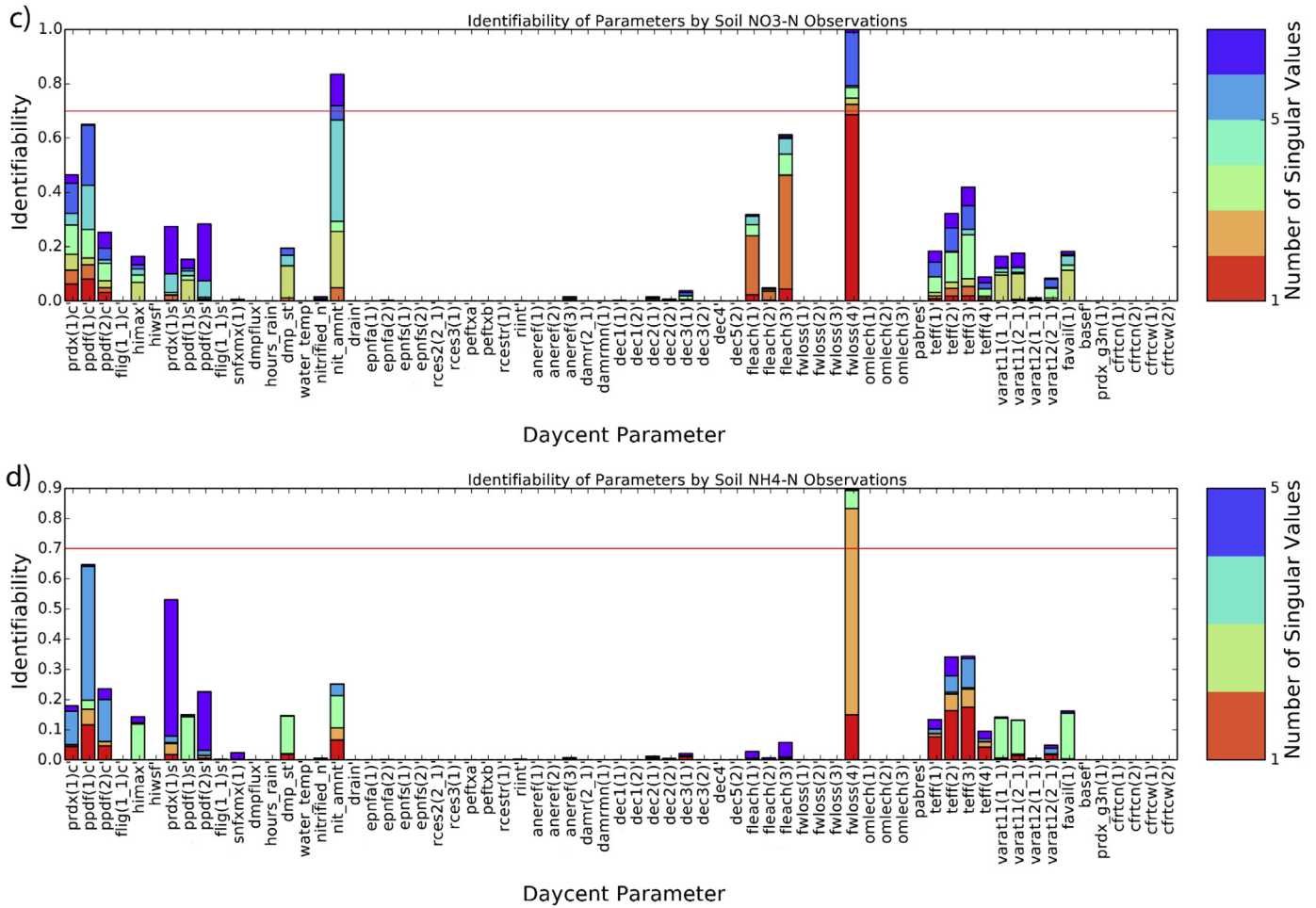
Fig. 4. (*continued*).

distribution of N in the soil may partially explain these incongruities in model performance. Nitrogen is concentrated in the area of the fertilizer application bands where both the soil cores (from which NO_3^-, NH_4^+ were measured) and the static chamber N_2O gas samples were collected. There are multiple ways in which the spatial variation of a complex three-dimensional soil system cannot be perfectly represented in the one-dimensional representation of the soil column modeled in DayCent: a) fertilizer application at different soil depths is not represented; b) accounting for a higher areal fertilizer concentration in the application band cannot perfectly reflect lateral and vertical N-transport in the soil; c) soil samples might not be representative of the soil under the static chambers, and this may contribute to measurement error, that has not been quantified due to an insufficient number of replicates. It is likely that because N mineralization was limited (Table 2), there was insufficient available N to meet the modeled demand for crop growth, N_2O production and match observed soil N levels. Also, since N_2O fluxes following fertilization events dominate annual cumulative N_2O flux (e.g., Jacinthe and Dick, 1997), underestimation of N_2O flux after fertilizer addition leads to incorrect annual flux. A tendency of DayCent to underestimate very high N_2O fluxes has been previously observed (US EPA, 2014). An underestimation of all N vectors exclusively during the short period after fertilization suggested that there is a need to improve the model representation of highly fertilized field conditions, e.g., by providing options for fertilizer applications at varying soil depths.

4.2. Estimated parameter values and parameter correlations

Parameter identifiability reflects the amount of information contained in the observations used for calibration and when information content is low there is a tendency to estimate unreasonable parameters values (Poeter and Hill, 1997). In this analysis, the calibration dataset contained information sufficient to accurately identify 16 parameters; the values of the remaining estimated parameters were accompanied by considerable estimation error. This points out that the identifiability of the selected parameters in the present study has been limited by the information contained in the observations. A dataset containing additional observation types and representing a wider range of conditions would provide additional information about the parameter values.

Estimated parameter values are simply those values that produce the best fit of the model to the observations, and as a result estimated values may alter relationships in unexpected ways that do not conform to our understanding of process function. In this study, however, a review of estimated parameter values and model outputs indicated that the parameter values were reasonable and that the calibrated model represented the agro-ecosystem and its underlying processes reasonably well over the simulated period. For example, although adjustments of the *ppdf* parameters intensified crop production within a narrowed temperature range, these changes did not delay the onset of corn and soybean growth in spring compared to the default simulation (Fig. 2a).
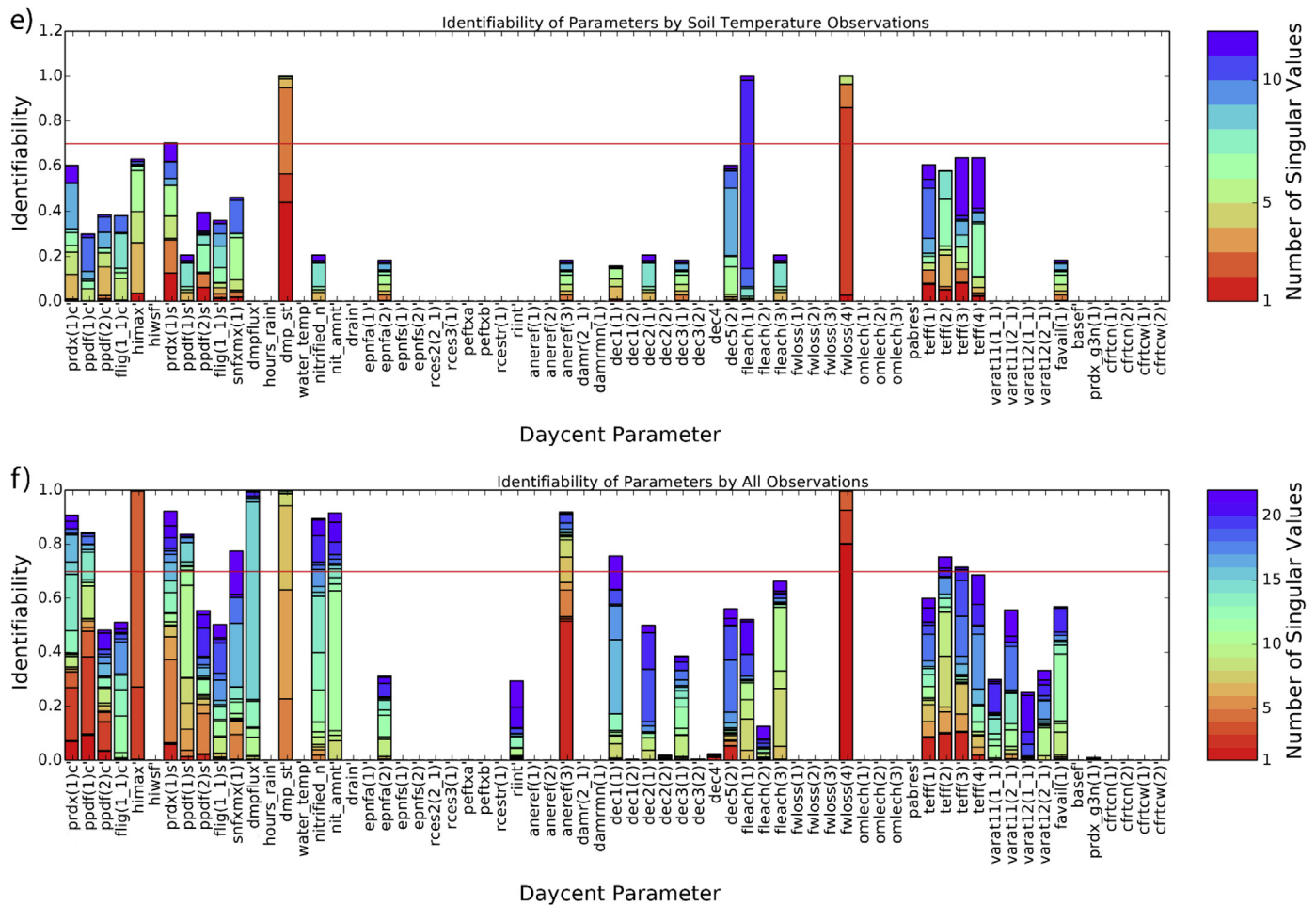
Fig. 4. (_continued_).

Correlation analysis revealed a few pairs of strongly correlated model parameters. Inclusion of a large number of parameters in inverse modeling often leads to some parameters being highly correlated (Doherty and Hunt, 2010a). Strong correlations among parameters indicate that a variety of combinations of parameter values can have the same impact on simulated values (Poeter and Hill, 1997). Similarly, when there is a strong correlation, changes in one parameter can be offset by changes in other parameters (Doherty and Hunt, 2009). The values of the parameter correlation coefficients can be positive or negative; this implies that an increase in the values of some parameters can have a similar effect on the simulated variables as an increase or decrease in the values of correlated parameters according to the direction of correlation. The strong correlations observed revealed that: a) parameters describing the maximum decomposition rate of SOM with slow turnover (_dec4_) and impact of soil anaerobic conditions on the maximum decomposition rate (_aneref(3)_) have very similar, but reverse effects on simulated SOC; parameters describing the temperature effect on decomposition (_teff(2)_, _teff(3)_) have similar effects on simulated SOC, N_2O, NO_3^-, and NH_4^+; parameters describing the lignin content of aboveground corn and soybean biomass (_flig(1,1)c_ and _flig(1,1)s_) have equivalent, but opposite effects on simulated NO_3^-, NH_4^+, and N_2O; _flig(1,1)c_ and the parameter that describes the maximum C/N ratio for material entering the active SOM pool (_varat12(1,1)_) has nearly equal but opposite effects on simulated N_2O. These last two pairs of correlated parameters affect simulated values through their control over

partitioning of organic matter pools. While lignin content influences the splitting of plant residues into structural (resistant) and metabolic (readily decomposable) pools, the C/N ratio controls the flows from structural and metabolic pools to the active SOM pool (Parton et al., 1993). The strong correlations (r > 0.95) indicate that these parameters are generally not uniquely estimable (Poeter and Hill, 1997), although SVD transforms the problem such that information is spread among the correlated parameters and a conditionally unique solution is attained.

The estimation process does not account for the influence of errors in the values of model parameters that were not included in the estimation set. Including additional parameters into the parameter estimation process would most likely change the behavior of the model to some degree, produce different estimated parameter values and result in additional parameter correlations. However, an effort was made to include all important model parameters, based on the judgment of model developers and past experience, and the number of parameters that can be estimated simultaneously is limited only by the amount of information available in the observations.

4.3. Parameter sensitivities and identifiability

Relative composite sensitivities quantify the effects of the parameters on the estimation process and identify those parameters with the largest influence on the simulated outputs. Sensitivity of some of the parameters to the model outputs was anticipated as
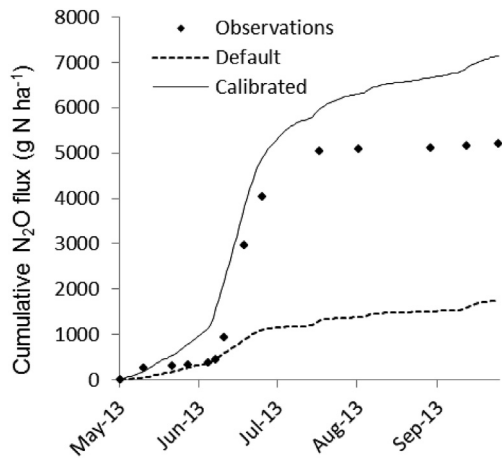
Fig. 5. Simulated and observed cumulative N$_2$O (g N/ha) fluxes during the validation period.

their sensitivity have been previously reported (e.g., Del Grosso et al., 2001, 2011; Parton et al., 1993; Rafique et al., 2013); sensitivity of others was unexpected but can be explained by their indirect effects on simulated outputs through model dynamics. In revealing these unexpected relationships inverse modeling helps users to better understand their model's structure and provides insights into how the model functions.

In DayCent, crop productivity is constrained by both soil temperature and water content. The temperature limitation is represented by a function defined by the optimum and maximum temperature parameters (*ppdf(1)c, ppdf(2)*), and the soil water content constraint is calculated as a function of the ratio of the sum of the amount of the rainfall, irrigation and stored water content to the potential evapotranspiration rate (*fwloss(4)*) (Del Grosso et al., 2001). These relationships explain the high sensitivity of these parameters to crop productivity.

The flows of C in the decomposition submodel are controlled by the inherent maximum decomposition rate of the different pools as well as by a water- and temperature-controlled decomposition factor (DEFAC) (Parton et al., 1993). These relationships explain the sensitivity of parameters which control calculation of soil temperature (*dmp_st*), the temperature effect on DEFAC (*teff(3),teff(2),-teff(4),teff(1)*), and the maximum decomposition rate of SOM with slow and intermediate turnover (*dec4, dec5(2)*) to SOC. The crop growth parameters (*ppdf(1)s, ppdf(2)s,* and *snfxmx(1)*) influence SOC indirectly through their effects on the amount of C entering the SOM pools from dead plants, which is a function of plant NPP.

Soil water content is calculated from the amount of rainfall that is intercepted by vegetation and litter and evaporated at the potential evapotranspiration rate. The amount of rainfall intercepted is a function of total rainfall, aboveground plant biomass and litter mass (Del Grosso et al., 2001). The sensitivity to VSWC of potential evapotranspiration rate (*fwloss(4)*), crop productivity parameters (*ppdf(1)c, ppdf(2)c, ppdf(1)s, ppdf(2)s, snfxmx(1)*), and also *dmpflux* which calculates soil water flow downwards as a function of hydraulic conductivity, is thus explained. However, the sensitivity to VSWC of the parameters that determine the effect of soil temperature on the decomposition rates (*teff(3),teff(2),teff(4), teff(1)*) is difficult to explain based on our understanding of the systems involved and the function of the DayCent model. Unexplained relationships like this should be explored further by examining how the relationships between soil temperature and decomposition rates are implemented in the model. Counter-intuitive results of this sort signal opportunities to improve our understanding of the

governing physical relationships or to correct an error in how those relationships are represented in the model.

Similarly, soil temperature in each soil layer is a function of air temperature, snow cover, plant biomass and litter. Increases in snow cover, plant biomass and litter lead to soil temperature being less responsive to changes in air temperature (Del Grosso et al., 2001). This clarifies the sensitivity to soil temperature of parameters affecting calculation of crop productivity (*ppdf(2)s, ppdf(2)c, snfxmx(1)*), however it does not explain the sensitivity of parameters governing the effect of temperature on decomposition (*teff(3), teff(2), teff(1),teff(4)*) or *epnfa(2)* (wet and dry N deposition). Since *epnfa(2)* is involved in calculation of atmospheric external N inputs, including non-symbiotic N fixation, we presume its sensitivity may be connected to the sensitivity of *snfxmx(1)*.

Simulated N$_2$O emissions are a product of both nitrification and denitrification (Del Grosso et al., 2001). The logic of sensitivity of the maximum daily nitrification rate parameter, *nit_amnt*, to N$_2$O flux is self-evident. Nitrification rate is a function of soil temperature until it reaches the average high temperature of the warmest month of the year; thus explaining the high sensitivity of the damping factor of soil temperature (*dmp_st*). The sensitivities of parameters describing soil N availability to plants (*favail(1)*), the temperature effect on crop growth and consequently the amount of N uptake by the crop (*ppdf(1)c, ppdf(1)s, ppdf(2)s*), are related to denitrification and nitrification rates that are functions of soil NO$_3^-$ and NH$_4^+$, respectively. Additionally, nitrification is limited by soil water stress on microbial activity when soil water content is low and by oxygen availability when soil moisture is high (Del Grosso et al., 2001). In contrast, calculated denitrification rates are limited by oxygen availability, which is controlled by soil water content. The high sensitivity of potential evapotranspiration (*fwloss(4)*) to N$_2$O flux thus results from its key role in the soil water balance. The sensitivity of parameters describing the temperature effect on decomposition rates (*teff(3),teff(2),teff(4), teff(1)*), and maximum and minimum C/N ratio of decomposing biomass entering surface SOM (*varat11(1,1), varat11(2,1)*) is related to their effects on the transfer of nutrients from dead plant material to the active SOM pool, its decomposition, further ammonification and consequently substrate availability to nitrification and denitrification. The sensitivity analysis yielded different outcomes in comparison with results of Rafique et al. (2013) due to the different calibration approach. Rafique et al. (2013) used only one type of data for the model calibration.

Some parameters were found to be almost insensitive even though we anticipated they would have strong influence on the simulated values. Although the initial SOC pools were generated through a long term simulation of native prairie ecosystem, parameters that control the effect of solar radiation on productivity of prairie grasses (*prdx_g3n(1)*) and the fraction of C allocated to grass roots under stress conditions (*cfrtcn(1), cfrtcn(2), cfrtcw(1), cfrtcw(2)*), all had low sensitivity to SOC. Simulated SOC was much more sensitive to parameters describing the decomposition rates over the course of simulation than to the parameters driving C inputs over the 800 year period of permanent grassland, even though these parameters were necessary to bring the SOC to equilibrium (Fig. 2b). The sensitivity of parameters determining the effect of solar radiation on crop productivity (*prdx(1)s, prdx(1)c*) was also very small. We hypothesize that a combination of NO$_3^-$ uptake, leaching and denitrification, may have created an N limitation to crop growth; thus explaining why the simulated crop productivity was fit to the observations by adjusting the temperature limitation growth parameters, rather than the *prdx* parameters that have limited sensitivity under nutrient stress conditions (Del Grosso et al., 2011).

High parameter identifiability indicates that the dataset or subset of observations possesses the information that is required to

resolve the value of the particular parameter, while parameter non-identifiability indicates an insufficiency of information. Identifiability on the basis of crop productivity and SOC was not evaluated due to the small number of observations available. Comparison of parameter identifiability using the other observation groups indicated that VSWC observations provided sufficient information to estimate the highest number of parameters, followed by soil temperature and N_2O observations. The NO_3^- and NH_4^+ observations were sufficient to identify only a very few parameters. Identifiability analysis indicated a large contribution of information by VSWC, soil temperature and N_2O measurements to the estimation of the parameters involved directly and indirectly in their calculation. Accurate measurements of these observations will allow the estimation of the values of parameters that influence them directly or indirectly with high certainty (Van Oijen et al., 2005). These findings may be important for future modeling efforts since VSWC and soil temperature measurements can be inexpensively obtained with a single instrument, are frequently measured during agronomic trials, but are rarely used in model calibration.

The identifiability of many DayCent parameters was shown to be consistent with their sensitivity. This is a well-established finding resulting from the similarities in computation of both statistics, extensively discussed by Hill (2010) and Doherty and Hunt (2010b). On the other hand, analysis revealed extensive parameter correlations affecting the identifiability of most of the highly sensitive parameters (Doherty and Hunt, 2009; Hill, 2010); e.g., the identifiability of the *teff(3)*, *snfxmx(1)*, *teff(2)*,*teff(4)*, *teff(1)* parameters on the basis of VSWC observations was reduced by correlations among them (i.e., correlation between *teff(2)* and *teff(3)*, *teff(2)* and *teff(4)*, *teff(3)* and *teff(4)*, and *snfxmx(1)*and *teff(1)*). This indicates that different combinations of the values of these parameters can lead to a similar model output thus limiting their independent estimation.

5. Conclusions

The inverse modeling approach can be used to calibrate several components of complex ecosystem biogeochemical models simultaneously. Its application here improved DayCent model performance in simulating crop productivity, SOC, VSWC, soil temperature, and N_2O emissions relative to the default DayCent simulation during both the calibration and validation period. Underestimation of the magnitude of pulses in soil NO_3^-, NH_4^+ and N_2O emissions after fertilization events suggests a need to improve the model representation of highly fertilized conditions.

Insights gained through inverse modeling improved our understanding of the relationships between DayCent model parameters and observations frequently collected during agronomic trials, which is important for model calibration using manual or inverse modeling techniques. Relative composite sensitivities compared the effects of 67 parameters on the simulated values of individual observation types identifying the key influential parameters that should be included in the model calibration process. Analysis of the parameter correlation structure identified sets of parameters that have a similar effect on the simulated values, indicating that their values cannot be uniquely estimated. Identifiability analysis compared the capabilities of five types of field observations to constrain the parameter values. Soil temperature and VSWC were identified as highly informative observations that should be collected and included in calibration of the DayCent model.

The use of inverse modeling has provided insights into the function of the DayCent biogeochemical model that cannot be obtained through normal use of the model for simulation or through manual model calibration procedures.

Models like DayCent are formal, quantitative representations of our understanding of how the physical world works. As such,

models codify hypotheses that can be tested through experimentation and comparison with observations. The inverse modeling process comprises a set of important tools for testing our understanding of system function as embodied in a model. The inverse modeling process systematically interrogates the model, explicating relationships that are not otherwise obvious to model users and developers. When the inverse model processes brings to light relationships that seem counter-intuitive, this is an opportunity to increase our understanding; reflecting either an error in how physical processes are represented in the model, errors in measurements of observation values, or the existence of relationships in the physical system that were unanticipated and the exploration of which may expand our understanding of the governing processes. Today, the iterative process of formulating our understanding of the world as a quantitative model and testing that model against physical observations is an essential part of how we improve our understanding of complex natural systems. Inverse modeling tools are a powerful way to systematize and accelerate that process, thus improving our understanding of ecosystem biogeochemical processes.

References

Aster, R.C., Borchers, B., Thurber, C.H., 2005. Parameter Estimation and Inverse Problems. Elsevier Academic Press, Amsterdam.

Beck, M.B., Halfon, E., 1991. Uncertainty, identifiability and the propagation of prediction errors: a case study of Lake Ontario. J. Forecast. 10, 135–161.

Beven, K.J., Freer, J., 2001. Equifinality, data assimilation, and uncertainty estimation in mechanistic modeling of complex environmental systems. J. Hydrol. 249, 11–29.

Bitterlich, S., Durner, W., Iden, S.C., Knabner, P., 2005. Inverse estimation of the unsaturated soil hydraulic properties from column outflow experiments using free-form parameterizations. Vadose Zone J. 3, 971–981.

Bouwman, A.F., Boumans, L.J.M., Batjes, N.H., 2002. Emissions of N_2O and NO from fertilized fields: summary of available measurement data. Glob. Biogeochem. Cycles 16 (4), 1058.

Brilli, L., Moriondo, M., Bindi, M., 2013. Mediterranean savanna system: understanding and modeling of olive orchard. In: Geophysical Research Abstracts. EGU General Assembly 2013, Held 7-12 April, 2013 in Vienna, Austria, vol. 15 id. EGU2013–5432.

Cheng, K., Ogle, S.M., Parton, W.J., Pan, G., 2014. Simulating greenhouse gas mitigation potentials for Chinese Croplands using the DAYCENT ecosystem model. Glob. Change Biol. 20, 948–962.

Conant, R.T., Paustian, K., 2002. Spatial variability of soil organic carbon in grasslands: implications for detecting change at different scales. Environ. Pollut. 116 (1), S127–S135.

Del Grosso, S.J., Parton, W.J., Mosier, A.R., Hartman, M.D., Brenner, J., Ojima, D.S., Schimel, D.S., 2001. Simulated interaction of carbon dynamics and nitrogen trace gas fluxes using the DAYCENT model. In: Schaffer, M., Ma, L., Hansen, S.

(Eds.), Modeling Carbon and Nitrogen Dynamics for Soil Management. CRC Press, Boca Raton, Florida, pp. 303—332.

Del Grosso, S.J., Ojima, D.S., Parton, W.J., Mosier, A., Peterson, G., Schimel, D., 2002. Simulated effects of dryland cropping intensification on soil organic matter and greenhouse gas exchanges using the DAYCENT ecosystem model. Environ. Pollut. 116 (S1), S75—S83.

Del Grosso, S.J., Mosier, A.R., Parton, W.J., Ojima, D.S., 2005. DAYCENT model analysis of past and contemporary soil N_2O and net greenhouse gas flux for major crops in the USA. Soil Tillage Res. 83, 9—24.

Del Grosso, S.J., Halvorson, A.D., Parton, W.J., 2008a. Testing DAYCENT model simulations of corn yields and nitrous oxide emissions in irrigated tillage systems in Colorado. J. Environ. Qual. 37 (4), 1383—1389.

Del Grosso, S.J., Parton, W.J., Ojima, D.S., Keough, C.A., Riley, T.H., Mosier, A.R., 2008b. DAYCENT simulated effects of land use and climate on county level N loss vectors in the USA. In: Follett, R.F., Hatfield, J.L. (Eds.), Nitrogen in the Environment: Sources, Problems, and Management, second ed. Elsevier Science Publishers, The Netherlands, pp. 571—595.

Del Grosso, S.J., Ojima, D.S., Parton, W.J., Stehfest, E., Heistemann, M., DeAngelo, B., Rose, S., 2009. Global scale DAYCENT model analysis of greenhouse gas emissions and mitigation strategies for cropped soils. Glob. Planet. Change 67 (1—2), 44—50.

Del Grosso, S.J., Parton, W.J., Keough, C.A., Reyes-Fox, M., 2011. Special features of the DayCent modeling package and additional procedures for parameterization, calibration, validation, and applications. In: Ahuja, L.R., Ma, L. (Eds.), Methods of Introducing System Models into Agricultural Research. American Society of Agronomy, Madison, USA, pp. 155—176.

Doherty, J., 2003. Ground water model calibration using pilot points and regularization. Ground Water 41 (2), 170—177.

Doherty, J., 2005. PEST. Model-independent Parameter Estimation. User Manual, fifth ed. Watermark Numerical Computing, Brisbane, Australia.

Doherty, J., 2008. Manual and Addendum for PEST: Model Independent Parameter Estimation. Watermark Numerical Computing, Brisbane, Australia.

Doherty, J.E., Hunt, R.J., 2009. Two statistics for evaluating parameter identifiability and error reduction. J. Hydrol. 366, 119—127.

Doherty, J., 2010. PEST, Model-independent Parameter Estimation—User Manual (fifth ed., with slight additions). Watermark Numerical Computing, Brisbane, Australia.

Doherty, J.E., Hunt, R.J., 2010a. Approaches to Highly Parameterized Inversion—a Guide to Using PEST for Groundwater-model Calibration. U.S. Geological Survey Scientific Investigations Report 2010—5169. USGS, Madison, USA.

Doherty, J., Hunt, R.J., 2010b. Response to comment on "Two statistics for evaluating parameter identifiability and error reduction". J. Hydrol. 380 (3—4), 489—496.

Doherty, J., Welter, D., 2010. A short exploration of structural noise. Water Resour. Res. 46, W05525.

Fienen, M.N., 2013. We Speak for the Data. Groundwater. http://dx.doi.org/10.1111/gwat.12018.

Grant, R.F., Nyborg, M., Laidlaw, J.W., 1993. Evolution of nitrous-oxide from soil. 1. Model development. Soil Sci. 156, 259—265.

Hartman, M.D., Baron, J.S., Clow, D.W., Creed, I.F., Driscoll, C.T., Ewing, H.A., Haines, B.D., Knoepp, J., Lajtha, K., Ojima, D.S., Parton, W.J., Renfro, J., Robinson, R.B., Van Miegroet, H., Weathers, K.C., Williams, M.W., 2009. DayCent-chem Simulations of Ecological and Biogeochemical Processes of Eight Mountain Ecosystems in the United States. U.S. Geological Survey Scientific Investigations Report 2009—5150. USGS, USA.

Hill, M.C., Tiedeman, C.R., 2007. Effective Groundwater Model Calibration with Analysis of Data, Sensitivities, Predictions, and Uncertainty. John Wiley and Sons, Hoboken, NJ.

Hill, M.C., 2010. Comment on 'Two statistics for evaluating parameter identifiability and error reduction" by John Doherty and Randall J. Hunt. J. Hydrol. 380, 481—488.

Hunt, R.J., Doherty, J., Tonkin, M.J., 2007. Are models too simple? Arguments for increased parameterization. Ground Water 45 (3), 254—262.

Hunt, R.J., Luchette, J., Schreuder, W.A., Rumbaugh, J.O., Doherty, J., Tonkin, M.J., Rumbaugh, D.B., 2010. Using a cloud to replenish parched groundwater modeling efforts. Rapid Commun. Groundw. 48 (3), 360—365.

Jacinthe, P.-A., Dick, W.A., 1997. Soil management and nitrous oxide emissions from cultivated fields in southern Ohio. Soil Tillage Res. 41 (3—4), 221—235.

Kosugi, K., Mori, K., Yasuda, H., 2001. An inverse modelling approach for the characterization of unsaturated water flow in an organic forest floor. J. Hydrol. 246, 96—108.

Kladivko, E., Helmers, M., Abendroth, L., Herzmann, D., Lal, R., Catellano, M., Mueller, D., Sawyer, J., Anex, R., Arritt, R., Basso, B., Bonta, J., Bowling, L., Cruse, R., Fausey, N., Frankenberger, J., Gassman, P., Gassmann, A., Kling, K., Kravchenko, A., Lauer, J., Miguez, F., Nafzinger, E., Nkongolo, N., O'Neal, M., Owens, L., Owens, P., Scharf, P., Shipitalo, M., Strock, J., Villamil, M., 2014. Standardized research protocols enable transdisciplinary research of climate variation impacts in corn production systems. J. Soil Water Conserv. 69 (6), 532—542.

Kravchenko, A.N., Robertson, G.P., 2011. Whole-profile soil carbon stocks: the danger of assuming too much from analyses of too little. Soil Sci. Soc. Am. J. 75, 235—240.

Lamers, M., Ingwersen, J., Streck, T., 2007. Modelling N_2O emission from a forest upland soil: a procedure for an automatic calibration of the biogeochemical model Forest-DNDC. Ecol. Model. 205, 52—58.

Li, C., Aber, J., Stange, F., Butterbach-Bahl, K., Papen, H., 2000. A process-oriented model of N_2O and NO emissions from forest soils: 1. Model development. J. Geophys. Res. 105, 4369—4384.

Lin, Z., Radcliffe, D.E., 2006. Automatic calibration and predictive uncertainty analysis of a semidistributed watershed model. Vadose Zone J. 5, 248—260.

Lin, Y.F., Anderson, M.P., 2003. A digital procedure for ground water recharge and discharge pattern recognition and rate estimation. Ground Water 41, 306—315.

Malone, R.W., Jaynes, D.B., Ma, L., Nolan, B.T., Meek, D.W., Karlen, D.L., 2010. Soil-test N recommendations augmented with PEST-optimized RZWQM simulations. J. Environ. Qual. 39 (5), 1711—1723.

Malone, R.W., Nolan, B.T., Ma, L., Kanwar, R.S., Pederson, C., Heilman, P., 2014. Effects of tillage and application rate on atrazine transport to subsurface drainage: evaluation of RZWQM using a six-year field study. Agric. Water Manag. 132, 10—22.

Metherell, A.K., Harding, L.A., Cole, C.V., Parton, W.J., 1993. CENTURY, Soil Organic Matter Model Environment. Technical Documentation. Agroecosystem Version 4.0, Great Plains System Research Unit, Technical Report No. 4. USDA-ARS, Fort Collins, Colorado, USA.

Mitchell, D., Castellano, M., Sawyer, J., Pantoja, J., 2013. Cover crop effects on nitrous oxide emissions: role of mineralizable carbon. Soil Sci. Soc. Am. J. 77, 1765—1773.

Moore, C., Doherty, J., 2005. Role of the calibration process in reducing mode predictive error. Water Resour. Res. 41 (5), W05020.

Moore, C., Doherty, J., 2006. The cost of uniqueness in groundwater model calibration. Adv. Water Resour. 29 (4), 605—623.

Moriasi, D.N., Arnold, J.G., Van Liew, M.W., Bingner, R.L., Harmel, R.D., Veith, T.L., 2007. Model evaluation guidelines for systematic quantification of accuracy in watershed simulations. Trans. ASABE 50 (3), 885—900.

Müllera, Ch, Martina, M., Stevensb, R.J., Laughlin, R.J., Kammann, C., Ottow, J.C.G., Jager, H.-J., 2002. Processes leading to N2O emissions in grassland soil during freezing and thawing. Soil Biol. Biochem. 34 (9), 1325—1331.

Nolan, B.T., Malone, R.W., Ma, L., Green, C.T., Fienen, M.N., Jaynes, D.B., 2011. Inverse modeling with RZWQM2 to predict water quality. In: Ahuja, L.R., Ma, L. (Eds.), Methods of Introducing System Models into Agricultural Research. American Society of Agronomy, Madison, USA, pp. 327—364.

Nolan, B.T., Puckett, L.J., Ma, L., Green, C.T., Bayless, E.R., Malone, R.W., 2010. Predicting unsaturated zone nitrogen mass balances in agricultural settings of the United States. J. Environ. Qual. 39 (3), 1051—1065.

Olander, L.P., Haugen-Kozyra, K., 2011. Using Biogeochemical Process to Models to Quantify Greenhouse Gas Mitigation from Agricultural Management Projects. Technical working group on agricultural greenhouse gases (T-AGG) supplemental report. Duke University, USA.

Parkin, T.B., 2008. Effect of sampling frequency on estimates of cumulative nitrous oxide emissions. J. Environ. Qual. 37 (4), 1390—1395.

Parton, W.J., Scurlock, J.M.O., Ojima, D.S., Gilmanov, T.G., Scholes, R.J., Schimel, D.S., Kirchner, T., Menaut, J.-C., Seastedt, T., Garcia Moya, E., Kamnalrut, A., Kinyamario, J.I., 1993. Observations and modeling of biomass and soil organic matter dynamics for the grassland biome worldwide. Glob. Biogeochem. Cycles 7 (4), 785—809.

Parton, W.J., Rasmussen, P.E., 1994. Long term effects of crop management in wheat fallow: II. CENTURY model simulations. Soil Sci. Soc. Am. J. 58, 530—536.

Parton, W.J., Schimel, D.S., Ojima, D.S., Cole, C.V., 1994. A general model for soil organic matter dynamics: sensitivity to litter chemistry, texture and management. In: Bryant, R.B., Arnoldm, R.W. (Eds.), Quantitative Modeling of Soil Forming Processes. Soil Science Society of America, Madison, USA, pp. 147—167.

Parton, W.J., 1996. The CENTURY model. In: Powlson, D.S., Smith, P., Smith, J.U. (Eds.), Evaluation of Soil Organic Matter Models. Springer Berlin Heidelberg, pp. 283—291.

Parton, W.J., Hartman, M.D., Ojima, D.S., Schimel, D., 1998. DAYCENT: its land surface submodel: description and testing". Glob. Planet. Change 19, 35—48.

Parton, W.J., Holland, E.A., Del Grosso, S.J., Hartman, M.D., Martin, R.E., Mosier, A.R., Ojima, D.S., Schimel, D.S., 2001. Generalized model for NO_x and N_2O emissions from soils. J. Geophys. Res. 106, 17403—17419.

Parton, W.J., Morgan, J.,A., Wang, G., Del Grosso, S., 2007. Projected ecosystem impact of the Prairie Heating and CO_2 enrichment experiment. New Phytol. 1—12.

Parton, W.J., Hanson, P.J., Swanston, C., Torn, M., Trumbore, S.E., Riley, W., Kelly, R., 2010. ForCent model development and testing using the Enriched Background Isotope Study experiment. J. Geophys. Res. 115, G04001.

Poeter, E.P., Hill, M.C., 1997. Inverse models: a necessary next step in ground-water modeling. Ground Water 35 (2), 250—260.

Rafique, R., Fienen, M.,N., Parkin, T.B., Anex, R., 2013. Nitrous oxide emissions from cropland: a procedure for calibrating the DayCent biogeochemical model using inverse modelling. Water Air Soil Pollut. 224, 1677.

Rahn, K.-H., Werner, C., Kiese, R., Haas, E., Butterbach-Bahl, K., 2012. Parameter-induced uncertainty quantification of soil N_2O, NO and CO_2 emission from Hoglwald spruce forest (Germany) using the Landscape DNDC model. Biogeoscience 9, 3983—3998.

Schreuder, W.A., 2009. Running BeoPEST. In: Proceedings of the 1st PEST Conference, November 2—4, 2009, Potomac, Md.

Schwarz, G.E., Hoss, A.B., Alexander, R.B., Smith, R.A., 2006. The SPAROW Surface Water Quality Model: Theory, Application, and User Documentation. USGS Techniques and methods report 6-B3. USGS, Reston, VA, USA.

Spohrer, K., Herrmann, L., Ingwersen, J., Stahr, K., 2006. Applicability of uni- and bimodal retention functions for water flow modelling in a tropical Acrisol. Vadose Zone J. 5, 48—58.

Snyder, C.S., Bruulsema, T.W., Jensen, T.L., Fixend, P.E., 2009. Review of greenhouse gas emissions from crop production systems and fertilizer management effects. Agric. Ecosyst. Environ. 133 (3), 247—266.

Tonkin, M.J., Doherty, J., 2005. A hybrid regularized inversion methodology for highly parameterized environmental models. Water Resour. Res. 41 (10), W10412.

Tonkin, M.J., Doherty, J., 2009. Calibration-constrained Monte Carlo analysis of highly parameterized models using subspace techniques. Water Resour. Res. 45, W00B10.

US EPA, 2014. Inventory of U.S. Greenhouse Gas Emissions and Sinks: 1990-2012 (April 2014). Report EPA 430-R-14–003. U.S. Environmental Protection Agency, Washington, DC, USA.

Van Oijen, M., Rougier, J., Smith, R., 2005. Bayesian calibration of process-based forest models: bridging the gap between models and data. Tree Physiol. 25, 915–927.

Wallach, D., Makowski, D., Wigington, J., Brun, F., 2014. Working with Dynamic Crop Models: Methods, Tools and Examples for Agriculture and Environment, second ed. Elsevier Science, Oxford, UK.

Wang, G., 2005. Agricultural drought in a future climate: results from 15 global climate models participating in the IPCC 4th assessment. Clim. Dyn. 25, 739–753.

Wrage, N., Velthof, G.L., van Beusichem, M.L., Oenemaa, O., 2001. Role of nitrifier denitrification in the production of nitrous oxide. Soil Biol. Biochem. 33 (12–13), 1723–1732.